Miniature comfort motor control reference design with SiP

User guide

Z8F80908226

About this document

Design overview

The user guide describes the Miniature comfort motor control reference design with SiP (REF_MINI_CMFRT_SIP) using the TLE9954QSW40-33 MOTIX™ MCU System in package (SiP). The 3-phase bridge driver TLE9954QSW40-33 is used for automotive motor control for example *brushless direct current (BLDC)* seat adjustment or auxiliary pumps and fans in thermal management systems. The reference design is designed to drive 100 W loads at a battery voltage of 12 V.

The guide includes the schematics of the design, electrical, thermal, and *electromagnetic compatibility (EMC)* measurements according to the CISPR25 standard.

Highlighted components

1. MOTIX™ MCU TLE9954QSW40-33
2. OptiMOS™ 7 IAUZN04S7N026
3. XENSIV™ TLE5572-AE04E1-R-E0001

Applications

- BLDC seat adjustment
- Auxiliary water pump
- Oil pump

Highlighted design aspects

- Space optimization
- Cost optimization
- Thermal optimization

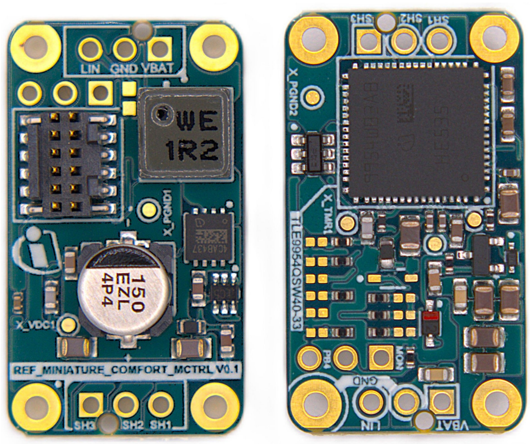

Figure 1 **Reference design**

Important notice

"Evaluation Boards and Reference Boards" shall mean products embedded on a printed circuit board (PCB) for demonstration and/or evaluation purposes, which include, without limitation, demonstration, reference and evaluation boards, kits and design (collectively referred to as "Reference Board").

Environmental conditions have been considered in the design of the Evaluation Boards and Reference Boards provided by Infineon Technologies. The design of the Evaluation Boards and Reference Boards has been tested by Infineon Technologies only as described in this document. The design is not qualified in terms of safety requirements, manufacturing and operation over the entire operating temperature range or lifetime.

The Evaluation Boards and Reference Boards provided by Infineon Technologies are subject to functional testing only under typical load conditions. Evaluation Boards and Reference Boards are not subject to the same procedures as regular products regarding returned material analysis (RMA), process change notification (PCN) and product discontinuation (PD).

Evaluation Boards and Reference Boards are not commercialized products, and are solely intended for evaluation and testing purposes. In particular, they shall not be used for reliability testing or production. The Evaluation Boards and Reference Boards may therefore not comply with CE or similar standards (including but not limited to the EMC Directive 2004/EC/108 and the EMC Act) and may not fulfill other requirements of the country in which they are operated by the customer. The customer shall ensure that all Evaluation Boards and Reference Boards will be handled in a way which is compliant with the relevant requirements and standards of the country in which they are operated.

The Evaluation Boards and Reference Boards as well as the information provided in this document are addressed only to qualified and skilled technical staff, for laboratory usage, and shall be used and managed according to the terms and conditions set forth in this document and in other related documentation supplied with the respective Evaluation Board or Reference Board.

It is the responsibility of the customer's technical departments to evaluate the suitability of the Evaluation Boards and Reference Boards for the intended application, and to evaluate the completeness and correctness of the information provided in this document with respect to such application.

The customer is obliged to ensure that the use of the Evaluation Boards and Reference Boards does not cause any harm to persons or third party property.

The Evaluation Boards and Reference Boards and any information in this document is provided "as is" and Infineon Technologies disclaims any warranties, express or implied, including but not limited to warranties of non-infringement of third party rights and implied warranties of fitness for any purpose, or for merchantability.

Infineon Technologies shall not be responsible for any damages resulting from the use of the Evaluation Boards and Reference Boards and/or from any information provided in this document. The customer is obliged to defend, indemnify and hold Infineon Technologies harmless from and against any claims or damages arising out of or resulting from any use thereof.

Infineon Technologies reserves the right to modify this document and/or any information provided herein at any time without further notice.

Table of contents

Table of contents

1 System offerings

Infineon's system offering for automotive 3-phase motor control with TLE9954QSW40-33 System-in-Package device encompasses a range of components that work together to provide a comprehensive solution.

Key Components:

- **TLE9954QSW40-33 DUT board:** A robust hardware foundation for efficient integration with a MOTIX™ MCU TLE9954QSW40-33, a OptiMOS™ 7 MOSFET, on board debugger, and several other interfaces
- **REF_WATERPUMP_SiP:** An optimized *printed circuit board (PCB)* for size, thermal and *EMC* performance. It highlights the size and PCB cost improvements against a traditional gate driver with discrete MOSFETs
- **REF_MINI_CMFRT_SiP:** Compact automotive solution with Infineon's fully integrated System-in-Package, optimized for minimal PCB size, and faster time-to-market
- **MOTIX™ TLE994_5x SDK Evaluation edition:** Evaluation edition of Software Development Kit (SDK) for MOTIX™ TLE994x and 995x including Peripheral Driver Library (PDL), Code examples, and Device Configurator settings. CMSIS Pack file
- **Infineon Automotive Power Explorer:** The Infineon Automotive Power Explorer is a powerful tool designed to provide a comprehensive and detailed analysis of Infineon products, enabling users to make informed decisions and optimize their designs. It offers a range of analysis features that enable users to evaluate and compare the performance of different products under various operating conditions
- **MOTIX™ MCU Solution Designer** The MOTIX™ MCU Solution Designer is a graphical configuration tool to analyze, debug, and tune your motor control application. The intuitive *graphical user interface (GUI)* helps to develop a field-oriented motor control application based on Infineon's MOTIX™ MCU families

2 Two reference designs for two different purposes with MOTIX™ MCU TLE9954QSW40-33

There are two reference designs for TLE9954QSW40-33 in the list above. Both reference designs are designed very differently and serve very different purposes.

2.1 Value of moving from discrete MOSFETs to System-in-Package

The REF_WATERPUMP_SiP was designed as a 1 to 1 replacement for the REF_WATERPUMP150W. The REF_WATERPUMP150W uses the traditional architecture with MOTIX™ MCU TLE995x and OptiMOS™ 7 integrated half-brigde MOSFETs. The integration of the MOSFETs allows for different improvements on the *PCB* listed below:

- **Reduction of PCB area by 40%:** Both PCBs were designed for the identical water pump and identical feature set. On the REF_WATERPUMP_SiP, the unutilized PCB space was cut away to show the saving in PCB area which resulted in a 40% reduction in PCB area. At the same time, both reference designs are capable of driving 150 W of continuous power
- **Simplification of 4 layer PCB down to 2 layer PCB:** The easier layout of the REF_WATERPUMP_SiP allows a better PCB layout on only 2 layers. This results in a cheaper PCB
- **Simplified layout:** As the routing in the commutation path is already integrated in the package of the System-in-Package, the layout gets much easier. First-time-right design with optimized *EMC* performance can be achieved due to low parasitic inductance

Below figure shows both REF_WATERPUMP150W (left) and REF_WATERPUMP_SiP (right) side by side.

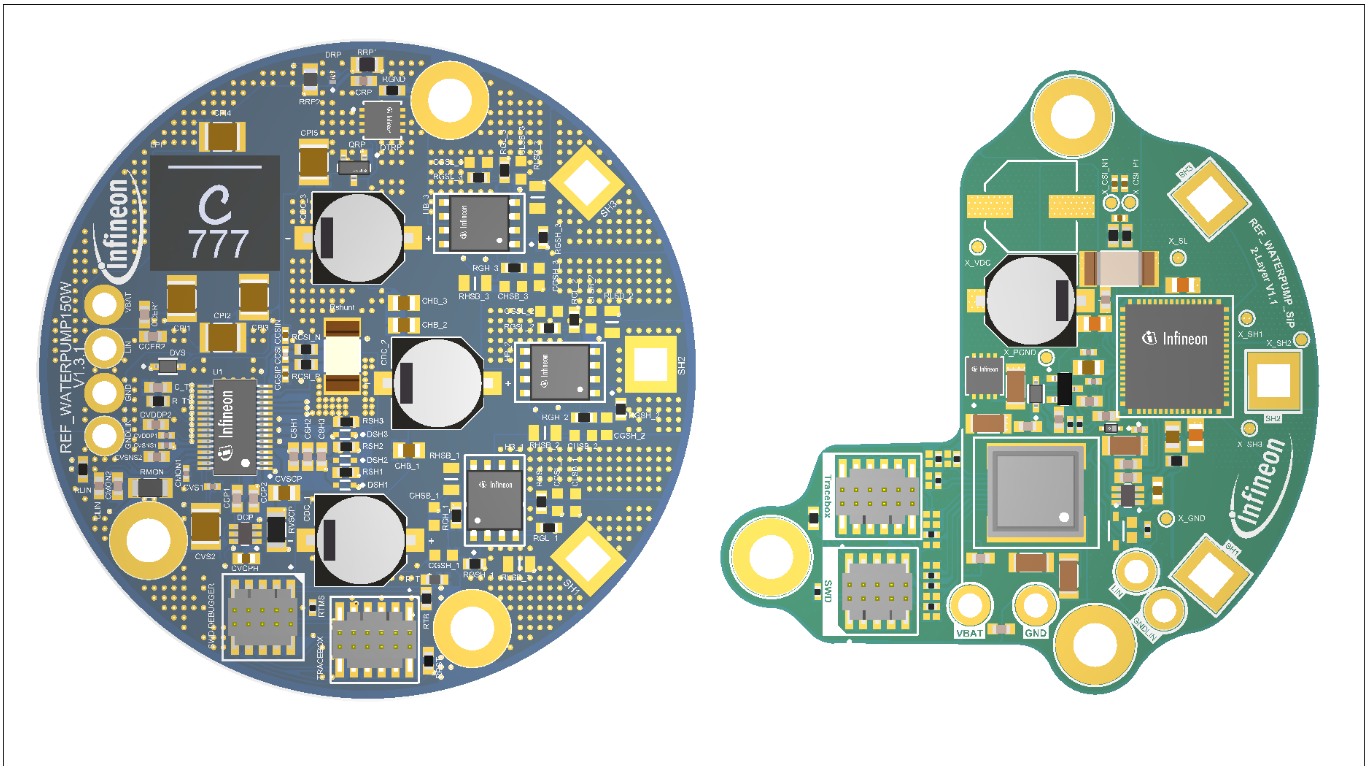

Figure 2 **Comparison of REF_WATERPUMP150W (left) and REF_WATERPUMP_SiP (right)**

For more details on the REF_WATERPUMP_SiP, refer to the board user guide of REF_WATERPUMP_SiP on the Infineon homepage.

2.2 Utilizing MOTIX™ MCU TLE9954QSW40-33 for extremely space constraint environments in comfort applications

Utilizing MOTIX™ MCU TLE9954QSW40-33 for extremely space constraint environments in comfort applications

The REF_MINI_CMFRT_SIP was designed to reduce the PCB size as much as possible. To achieve this small size of 30 mm x 17 mm, a double-sided assembly on a 4-layer board was utilized. The device is cooled via the topside of the mold compound of the MOTIX™ MCU TLE9954QSW40-33.

The figure below shows the REF_WATERPUMP_SiP (left) next to the REF_MINI_CMFRT_SIP (right) in correct relative scale.

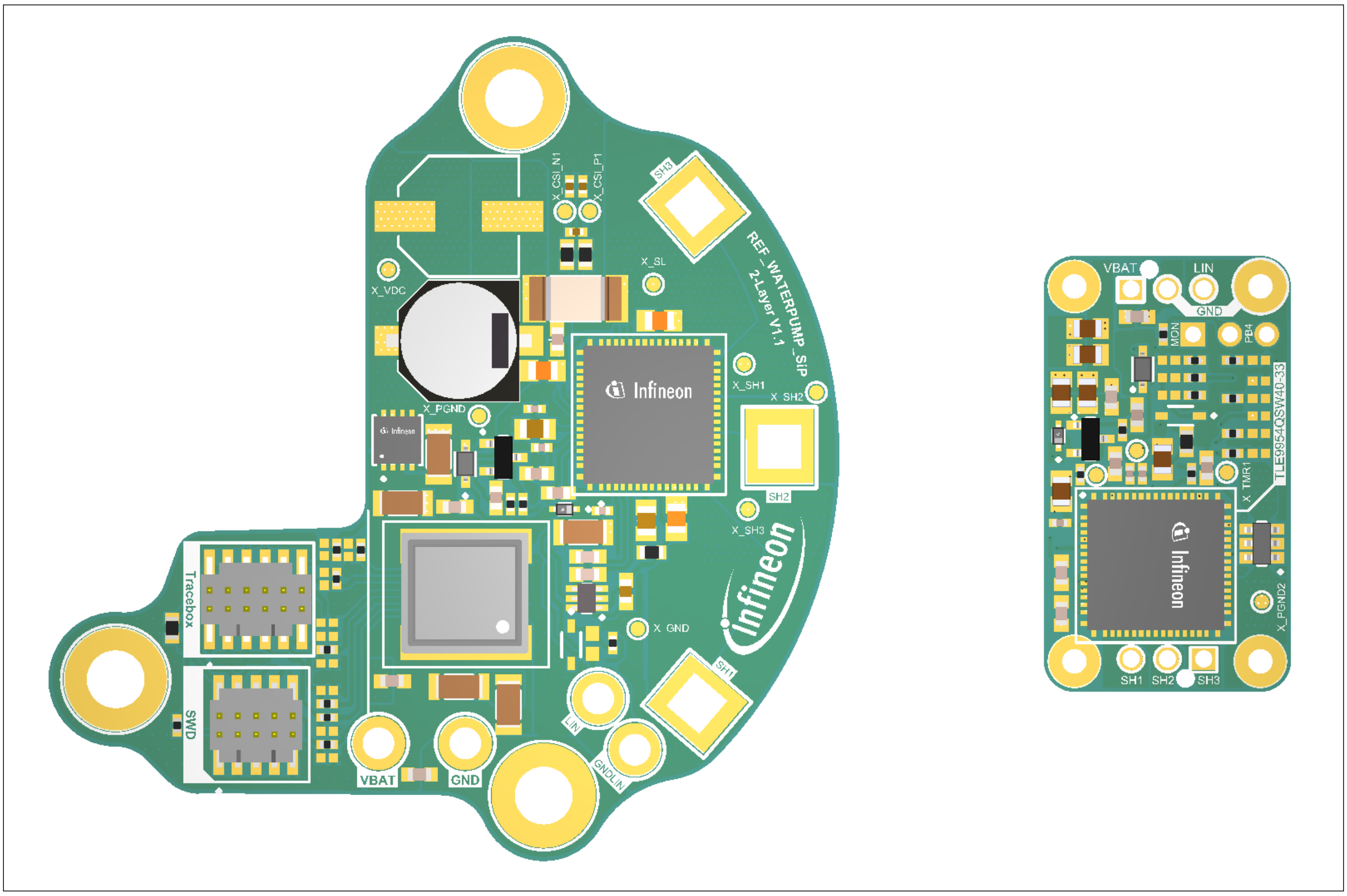

Figure 3 **Comparison of REF_WATERPUMP_SiP (left) and REF_MINI_CMFRT_SIP (right)**

To reduce the power losses even further, this design does not use a shunt resistor for current sensing. Instead, the XENSIV™ TLE5572 *tunnel magnetoresistance (TMR)* current sensor is used to measure the current flowing through the copper planes inside the PCB.

2.3 Key takeaway

The REF_MINI_CMFRT_SIP PCB showcases a highly compact PCB design enabled by the TLE9954QSW40-33 SiP. This user guide illustrates the performance capabilities of such a compact design, which features double-sided component placement optimized for top-side cooling, covering electrical and thermal characteristics as well as providing an initial indication of EMC behavior.

3 In detail: REF_MINI_CMFRT_SIP

The REF_MINI_CMFRT_SIP serves as a reference design for 100 W *brushless DC motor (BLDC motor)* comfort applications, such as BLDC motor seat adjustment, and can also be applied to other highly space constraint BLDC motor applications. The reference board has been developed using standard *PCB* materials and manufacturing processes.

The reference design features the MOTIX™ TLE9954QSW40-33 SiP, which integrates a B6-bridge. Additionally, it includes an OptiMOS™ 7 IAUZN04S7N026 MOSFET for reverse polarity protection. Power is supplied via a 12 V battery terminal connection. The design incorporates an input PI filter and supports *local interconnect network (LIN)* communication. Current measurement through the bridge is enabled by the XENSIV™ TLE5572 TMR current sensor. Furthermore, flash and debug communication with the microcontroller can be established through the provided debug connectors.

3.1 Design specifications

The design specifications are related to the assembled components and design considerations. They should not differ from the product datasheet recommendations. In case of deviations, the datasheet values of the products are valid.

Table 1 Design specifications

Parameter	Symbol	Values			Unit	Comment
		Min.	Typ.	Max.		
System parameters						
Function input voltage	V_{IN}	8	13.5	18	V	Specified by Design
Peak input current	I_{IN}	-	-	20	A	Peak current (<10 s)
Nominal input current	I_{IN}	-	8	-	A	2000 rpm
LIN interface	V_{BUS}	-40	-	40	V	
Phase voltage 1, 2, 3	V_{SH}	-8	-	48	V	
Thermal						
Operating temperature	T_A	-40	25	125	°C	Specified by design
Electromagnetic compatibility						
Conducted emissions				Class 4		CISPR25, 150 kHz-108 MHz
Mechanical specification						
Dimensions PCB	30 mm x 17 mm x 10mm (Width x Length x Height)					

3.2 Highlighted products

3.2.1 OptiMOS-7™ 40 V IAUZN04S7N026 MOSFET

A high-current, low $R_{DS(on)}$ power MOSFET in a 3x3 mm^2 advanced leadless package with a Cu-Clip for low package R_{ON} and minimal stray inductance, offering high power density, low conduction losses, and optimized switching behavior, with a reduced form factor compared to traditional leaded packages, ideal for automotive applications, for example power distribution, body control modules, and electric motors. For further information, see IAUZN04S7N026.

3.2.2 MOTIX™ MCU | 32-bit motor control SiP with integrated 3-phase bridge driver

TLE9954QSW40-33 belongs to the TLE995x family of 32-bit motor control SiPs with integrated 3-phase bridge driver and support for *LIN*. The potential applications of TLE995x include automotive motor control for auxiliary drives like pumps and fans in thermal management. In addition, *microcontroller unit (MCU)* system clock frequency supporting a wide range of motor control algorithms, either sensor-based or sensorless. Further information of the product can be found here.

3.2.3 XENSIV™ TLE5572-AE04E1-R-E0001

The XENSIV™ TLx5572 is a monocell *TMR*-based current sensor in a small and cost-competitive SOT23 package, which can replace a shunt and an OpAmp with a single component. The TLx5572 offers intrinsic isolation from the external current rail, with the benefit of reducing insertion resistance and allowing direct in-phase current measurement in automotive and industrial drives. And with its ultra-fast response time, it also provides a suitable solution for fast protection.

4 Hardware design guide

The battery supply of the reference design has an input PI filter and a reverse polarity protection circuit. The *direct current (DC)* link voltage (V_DC) is buffered via a combination of one hybrid and multiple ceramic capacitors. Further, the bridge driver TLE9954QSW40-33 is supplied by a 2-stage charge pump. The main component of the reference design, MOTIX™ SiP TLE9954QSW40-33, runs the motor control algorithm and drives the motor. Current measurement through the bridge is enabled by the XENSIV™ TLE5572 *TMR* current sensor. For debugging and flashing purposes, Tracebox and SWD Debug connectors are available.

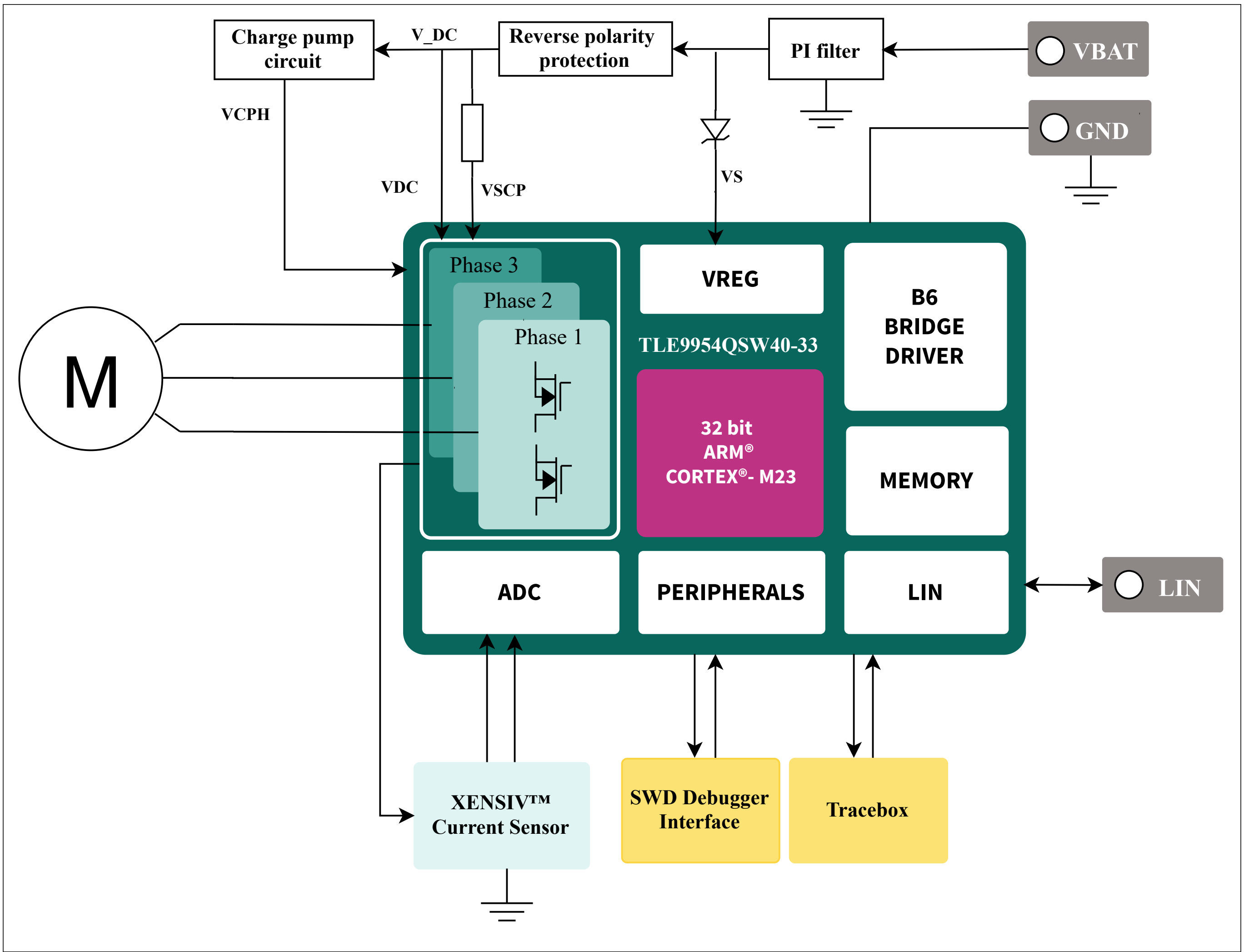

Figure 4 **Reference design overview**

4.1 General component selection

In general, the components for the reference design are selected to provide optimum performance. Wherever available, automotive-qualified components were selected. Further information about the components used can be found in the following sections.

4.2 Input filter and reverse polarity protection circuit

4.2.1 Input filter

The reference design has an on-board input filter. The filter used is a PI filter, which consists of ceramic input capacitors CPI1-3, a power inductor LPI and output capacitors CPI4-6. It is designed to filter the switching noise caused by *pulse-width modulation (PWM)* operation. The schematic and the component placement of the PI filter are depicted in the following figures.

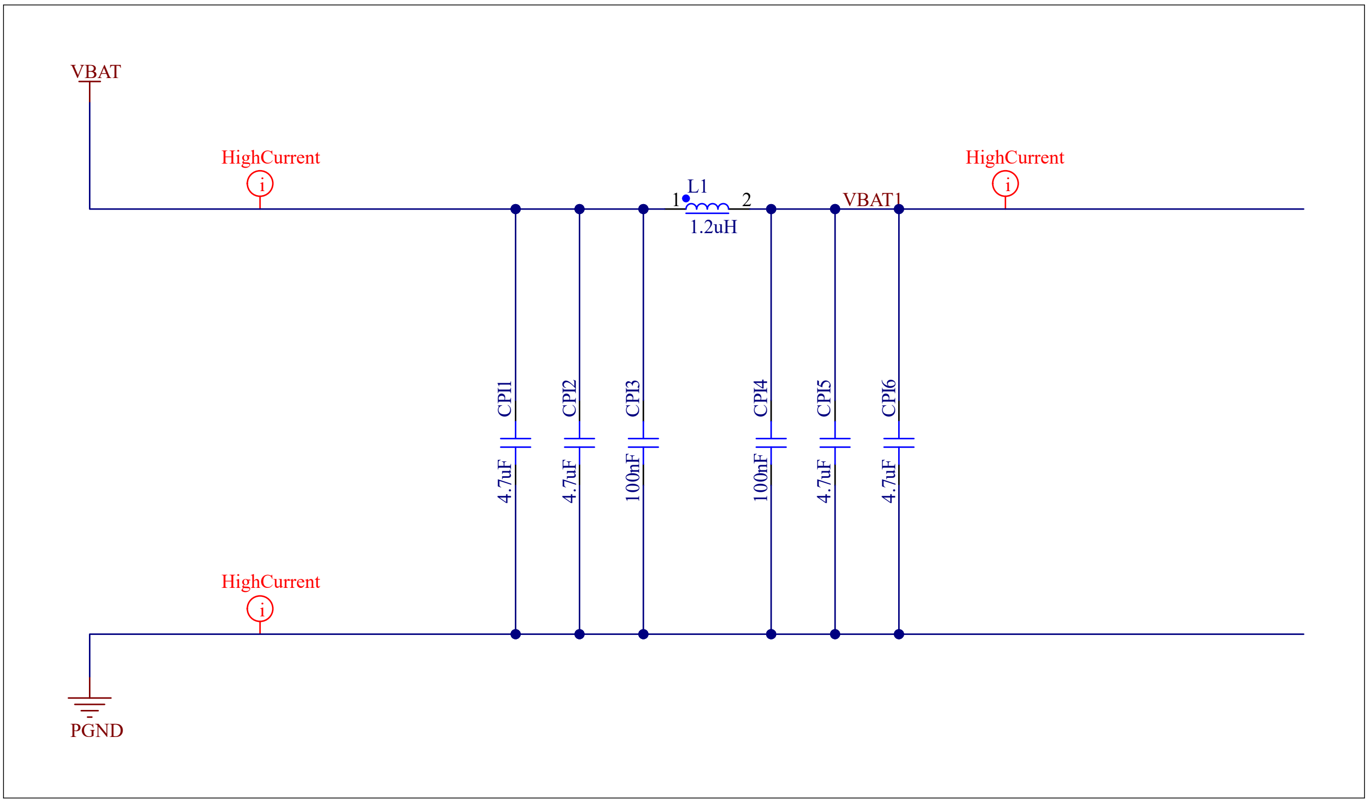

Figure 5 **PI-filter schematic**

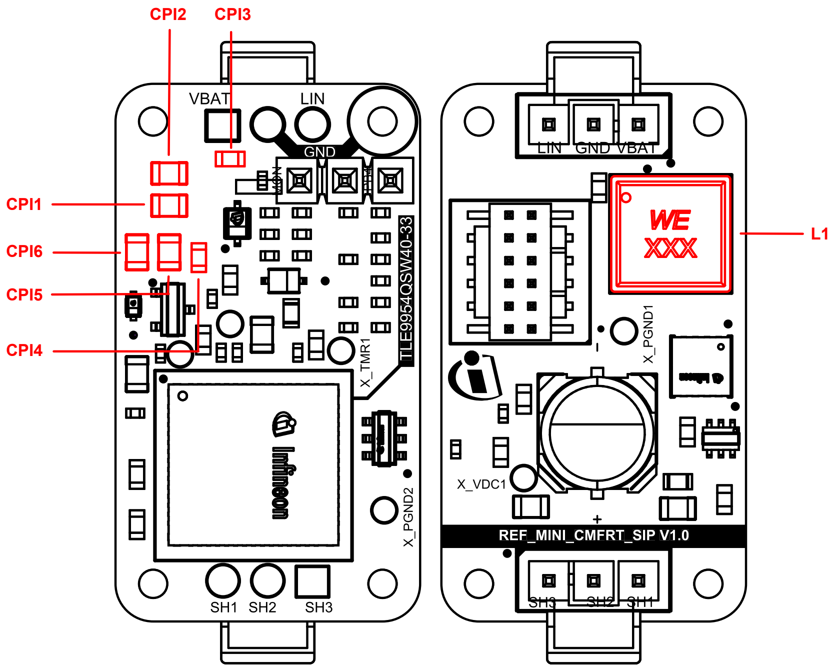

Figure 6 PI-filter component placement

4.2.2 Reverse polarity protection circuit

The reverse polarity protection is designed according to the Reverse Polarity Protection for Embedded Power ICs application note. The reverse polarity MOSFET Q1 (IAUZN04S7N026) is driven by the charge pump voltage VCPH as depicted in the reverse polarity circuit. The schematic and the component placement of the reverse polarity protection circuit are depicted in the following figures.

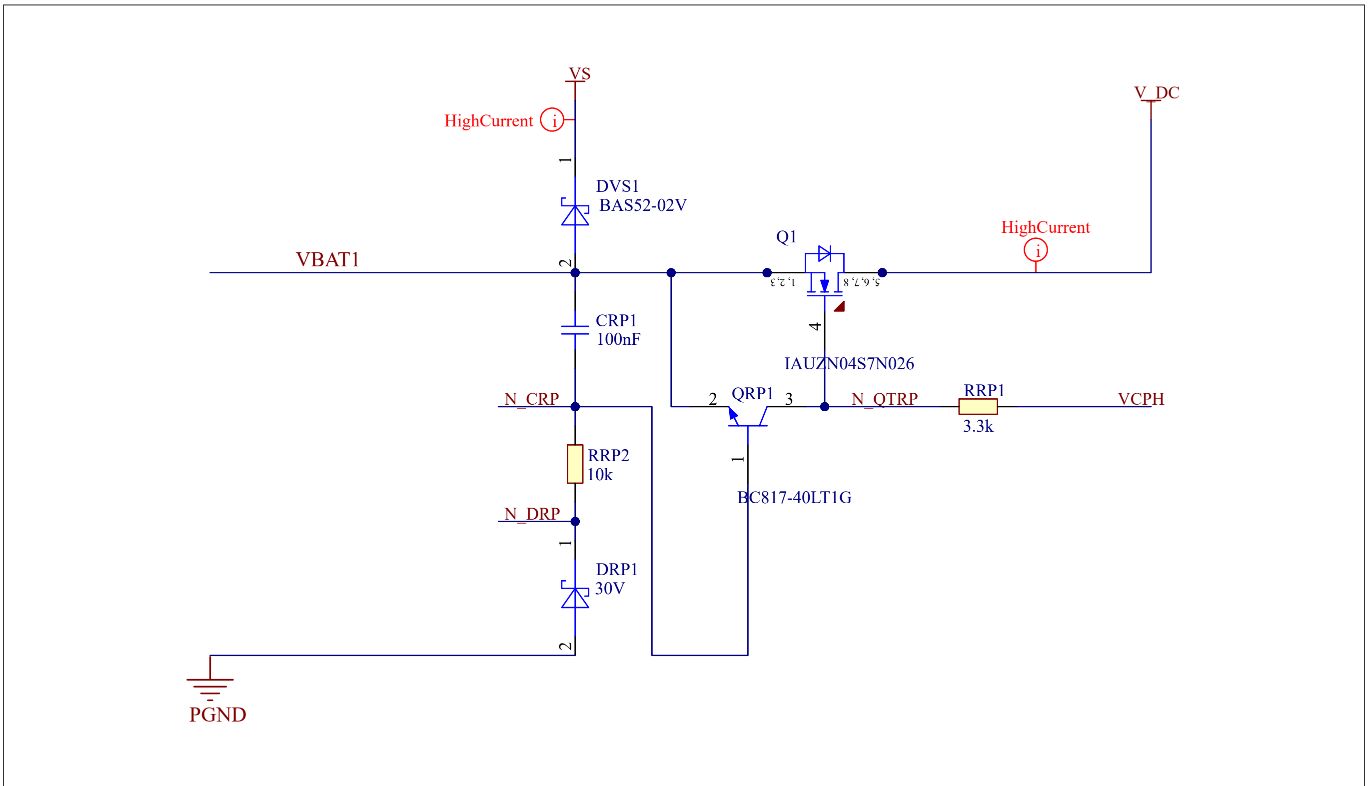

Figure 7 **Reverse polarity protection schematic**

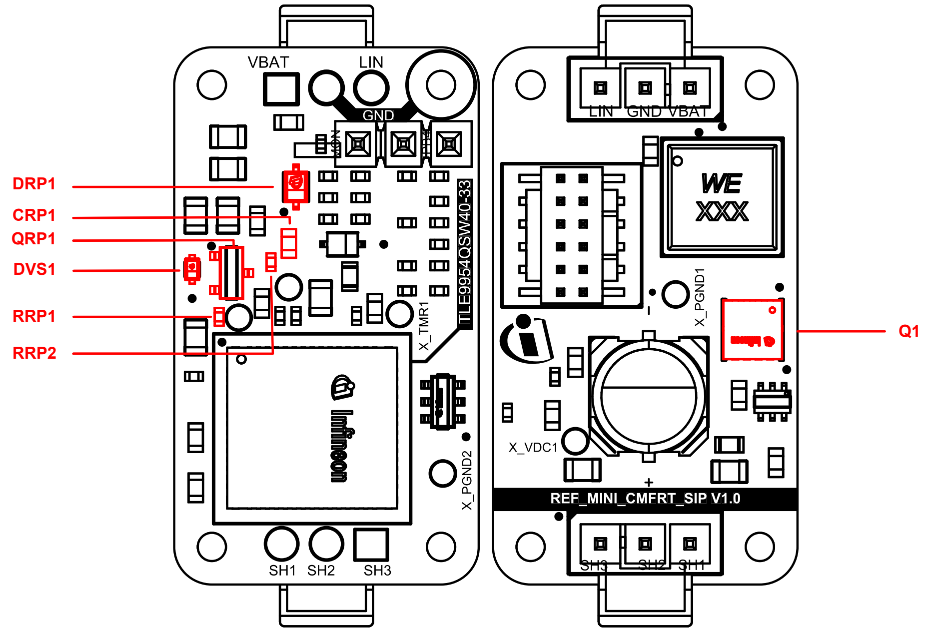

Figure 8 Reverse polarity protection component placement

4.3 Motor control components

4.3.1 Interfaces

The reference design features a Tracebox debug connector, allowing for effortless debugging and flashing of the device. The 12-pin Tracebox connector is specifically designed for use with Moteon's Tracebox and provides SWD, UART, and SPI signals. Notably, the UART and SPI pins can also be repurposed as generic *general purpose input output (GPIO)*s or utilized to connect external sensors, such as position sensors. It also enables connection to external debuggers such as Arm® Keil® ULINK or an XMC™ Link when using the provided adapter board. This connection enables the use of the MOTIX™ MCU solution designer to control the MOTIX™ motor control library during operation.

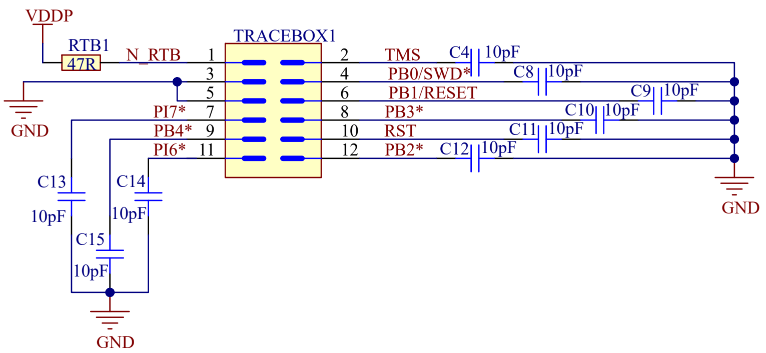

Figure 9 **Tracebox connector schematics with filter capacitor placement options. These capacitors are not populated by default**

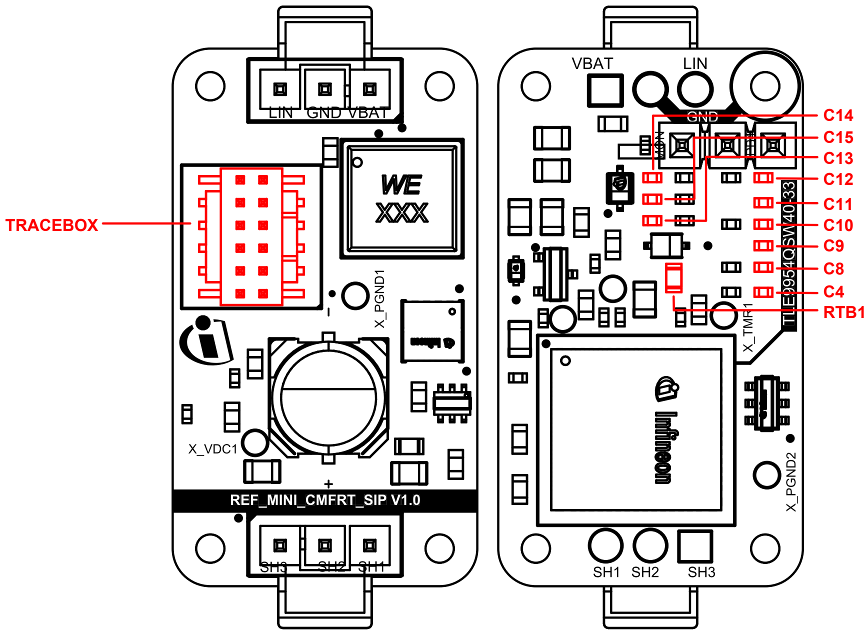

Figure 10 **Tracebox connector and component placement**

4.3.2 External components for MOTIX™ SiP TLE9954QSW40-33

4.3.2.1 Decoupling and buffer capacitors on supply pins

The decoupling and buffer capacitors are used to filter noise from the supply and provide a steady voltage to the circuit. The decoupling capacitors are ceramic capacitors with a typical value of 100 nF while the buffer capacitors have values that are application-dependent. The schematic and the component placement of the decoupling and buffer capacitors are depicted in the following figures.

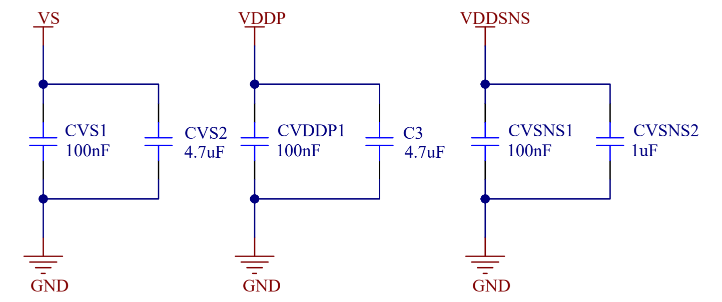

Figure 11 Decoupling and buffer capacitors schematic

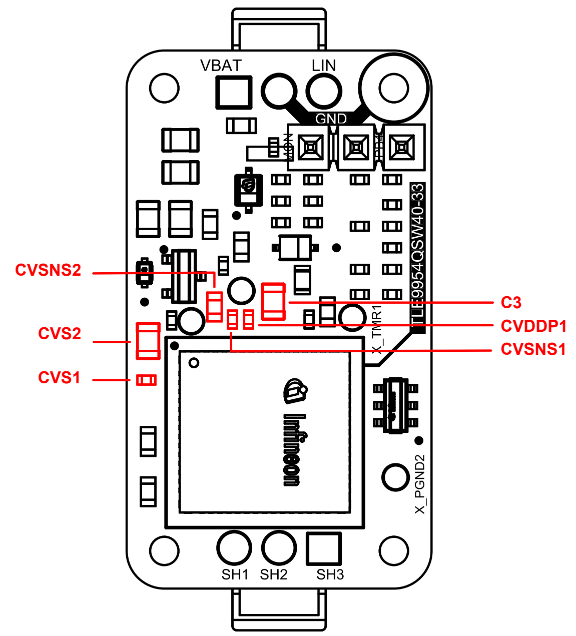

Figure 12 Decoupling and buffer capacitors component placement

4.3.2.2 Charge pump circuit

The bridge driver is supplied by a 2-stage charge pump for low-voltage operation and static MOSFET gate control. The default configuration of the charge pump requires two external buffer capacitors, two external flying capacitors, and four external diodes. The schematic and the component placement of the charge pump circuit are depicted in the following figures:

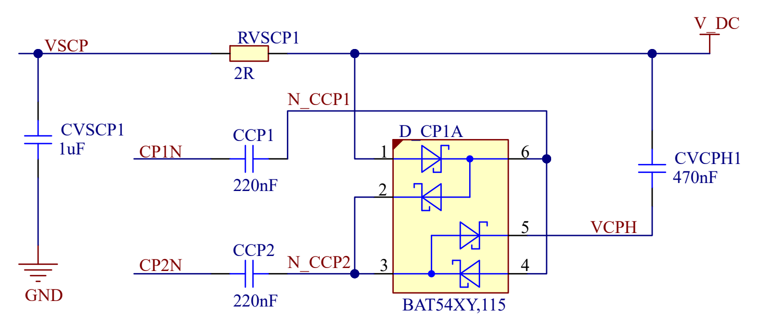

Figure 13 Charge pump circuit schematic

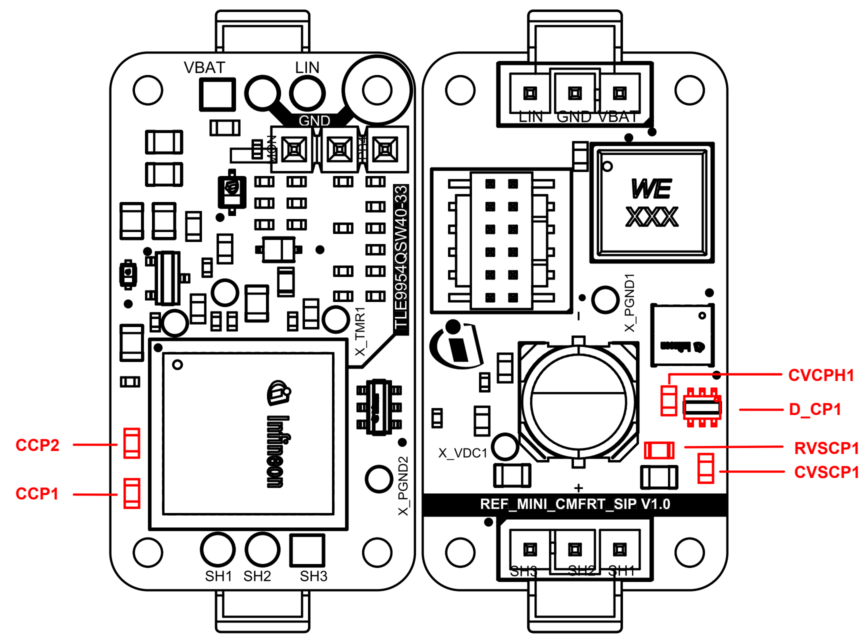

Figure 14 Charge pump circuit component placement

4.4 Power stage

4.4.1 DC-link capacitors

The board comes with a single 150 uF hybrid capacitor C5. There are two ceramic 4.7 uF capacitors placed between V_DC and SL left and right to give the best possible buffering as close as possible to the device during switching. The 100 nF capacitor is used for high-frequency switching noise. The schematic and the component placement of the *DC* link capacitors are depicted in the following figures:

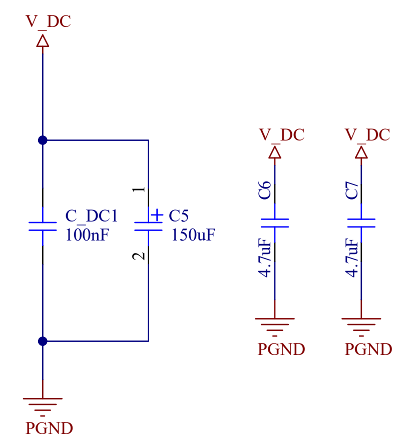

Figure 15 DC link capacitor schematic

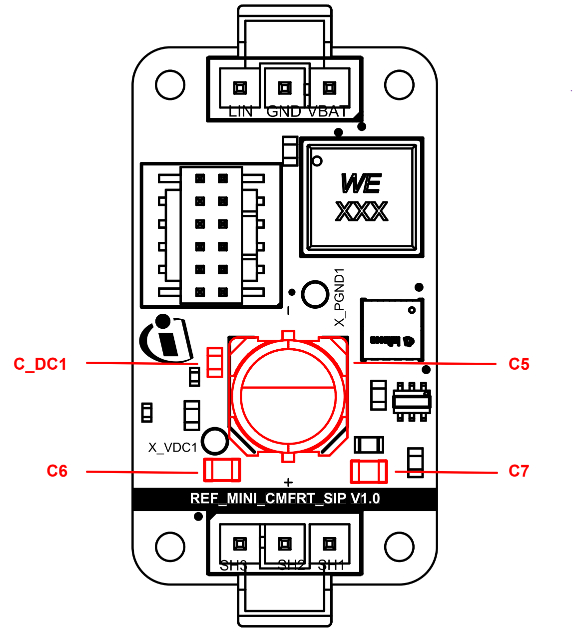

Figure 16 **DC link capacitor component placement**

4.4.2 Snubbers

Snubbers have not been used in the design. Due to the MOSFETs being integrated in the system package, there is no need for additional filter components. This comes from the very low parasitic inductance in the commutation path resulting in very good electrical and *EMC* characteristics. For further details, refer to System performance.

4.5 Measurement components

4.5.1 Current measurement via XENSIV™ TLE5572

For Motor current measurement, the XENSIV™ TLE5572 is used. It is a monocell *TMR*-based current sensor in a small and cost-competitive SOT23 package, which can replace a shunt and an OpAmp with a single component. The TLx5572 offers intrinsic isolation from the external current rail, with the benefit of reducing insertion resistance and allowing direct in-phase current measurement in automotive and industrial drives. With its ultra-fast response time, it also provides a suitable solution for fast protection.

The TLE5572 measures a magnetic field via a TMR bridge. The signal is fed into a first stage of amplification (OTA), and then through a high-bandwidth and high slew rate differential amplifier, which provides a single-ended output signal on the AOUT pin. The TLE5572 is supplied via the 5 V VDDSNS supply pin of TLE9954QSW40-33.

The AOUT output of the TLE5572 is connected to one of the 5 V analog inputs of the TLE9954QSW40-33, allowing the signal to be read out via the internal *analog-to-digital converter (ADC)*. A 0 Ω series resistance and 220 pF buffer capacitor are also provided, offering the option to filter the output signal if required.

The schematic and the component placement of the shunt measurement circuit are depicted in the following figures:

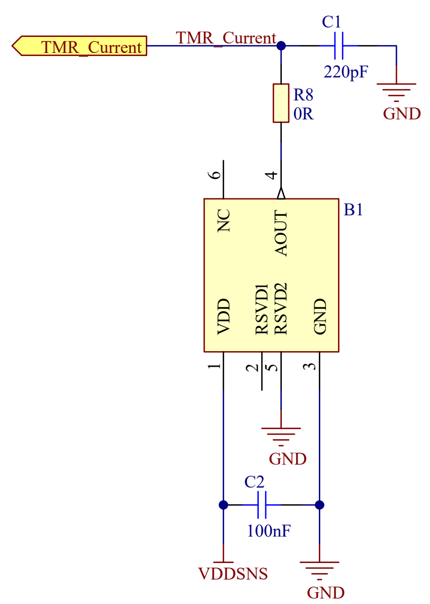

Figure 17 **XENSIV™ current sensor schematic**

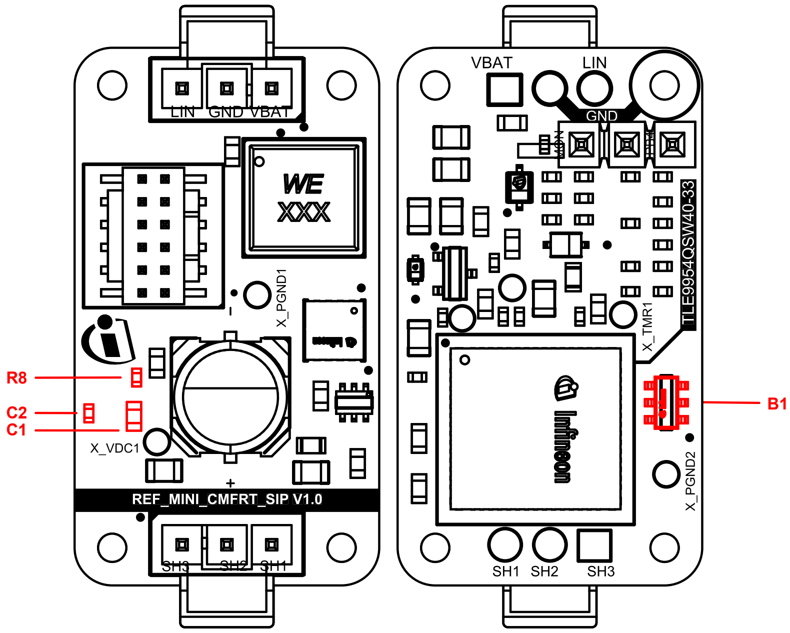

Figure 18 **XENSIV™ current sensor component placement**

5 Placement and layout

5.1 Components and interfaces

The reference design features a highly compact structure, minimizing *PCB* size while maintaining functionality. The battery terminals are located at the upper end of the board, alongside the *LIN* communication port. Either the provided connector or wires can be soldered to these ports. The 3-phase outputs of the motor bridge driver and corresponding phase terminals are situated at the bottom end of the board, with options to connect motor phases using the provided connector or individual wires. The Tracebox connector is located at the bottom side of the board, while the TLE9954QSW40-33 is positioned at the top side. To facilitate top-side cooling, all components on the top side are limited to a height of 1.4 mm or less. A limited number of test points are provided on both sides of the PCB for measuring switching signals. The PCB includes four mounting holes for mechanical assembly, such as attachment to a heat sink. The upper-right mounting hole is electrically connected to ground and marked with a white circle on the top side, allowing the PCB ground to be connected to the heat sink or motor ground, while the other mounting holes are electrically isolated from the rest of the circuit.

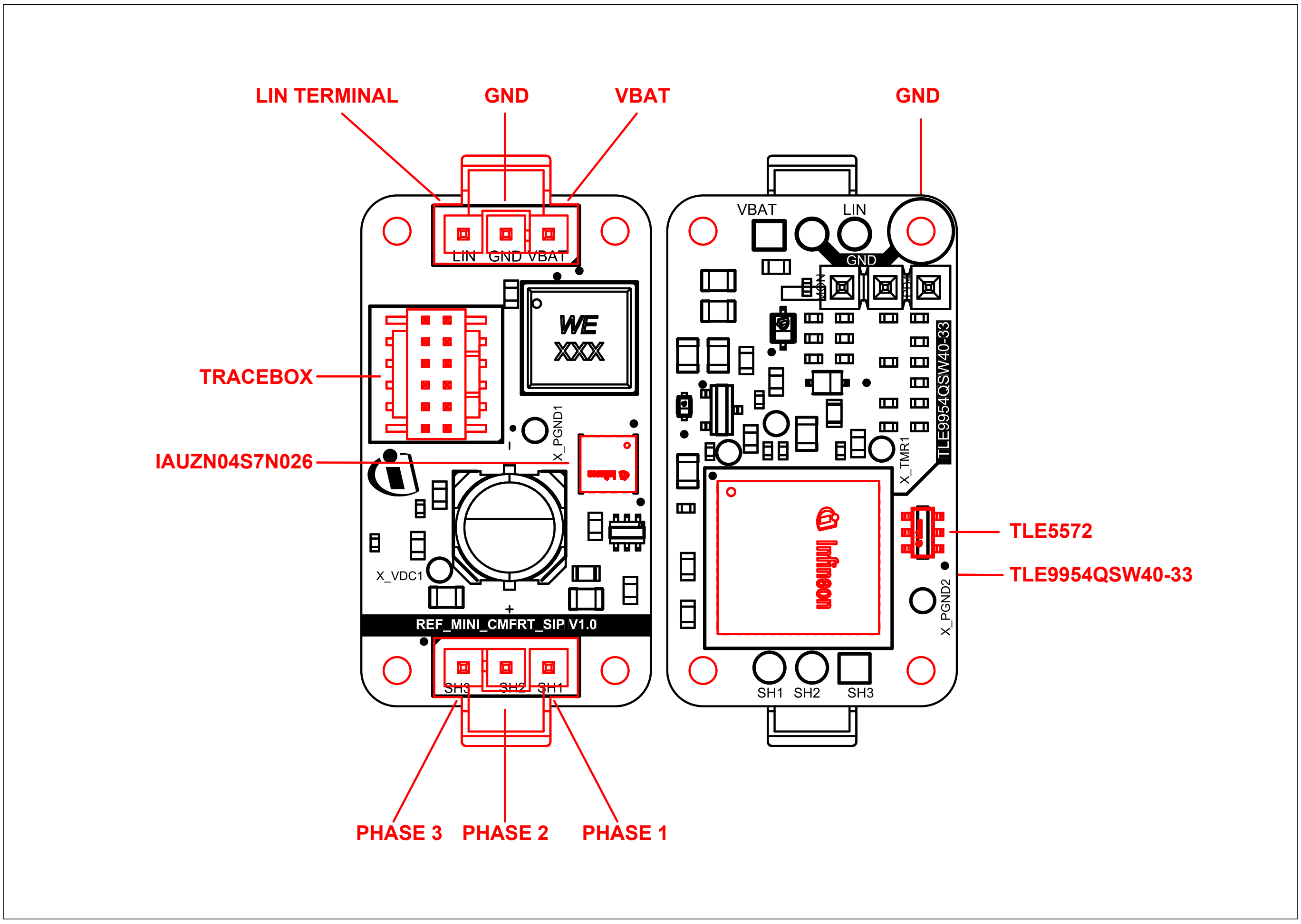

Figure 19 **Reference design**

6 Getting started with REF_MINI_CMFRT_SIP

Tool installation guide

To get the reference design ready and running, there are certain tools and software required. The software toolchain can be installed by following these instructions.

Content of the package

The box contains the following components:

- Miniature comfort motor control reference design with SiP
- Connector board
- Tracebox cable with 12-pin Tracebox connector
- 2x preassembled cables to connect *PCB* to power supply and Motor via Molex Nano-Fit connector
- 2x Molex Nano-Fit PCB header for assembly of Nano-Fit cables to PCB

Additional requirements

The following components are not part of the package and are needed additionally:

- MOTIX_MOTOR_BENCH or Nanotec DB42S03
- KIT_XMC_LINK_SEGGER_V1 isolated debug probe

Connecting the PCB for usage with Solution Designer

The reference design is powered by connecting the supply lines to the battery and *ground (GND)* terminals, which can be done either by soldering cables directly to the PCB or by using the provided MOLEX Nano-Fit connectors. To use the MOLEX Nano-Fit connectors, first solder the Nano-Fit PCB header to the PCB, then connect the supply lines to the MOLEX Nano-Fit connector. Similarly, the *BLDC motor* can be connected to the 3-phase output of the printed circuit board either by soldering its three phases directly to the PCB or by using the MOLEX Nano-Fit connectors. To establish a connection to a PC, use the connector board with an XMC™ Link. First, connect the Tracebox cable to the 12-pin Tracebox connector on the reference design and the DUT connector on the connector board. Then, connect the larger 8-pin connector on the XMC™ Link to the XMC_LINK_UART connector on the connector board. This setup enables flashing and debugging, as well as control of the motor control algorithm through the MOTIX™ MCU Solution Designer during runtime.

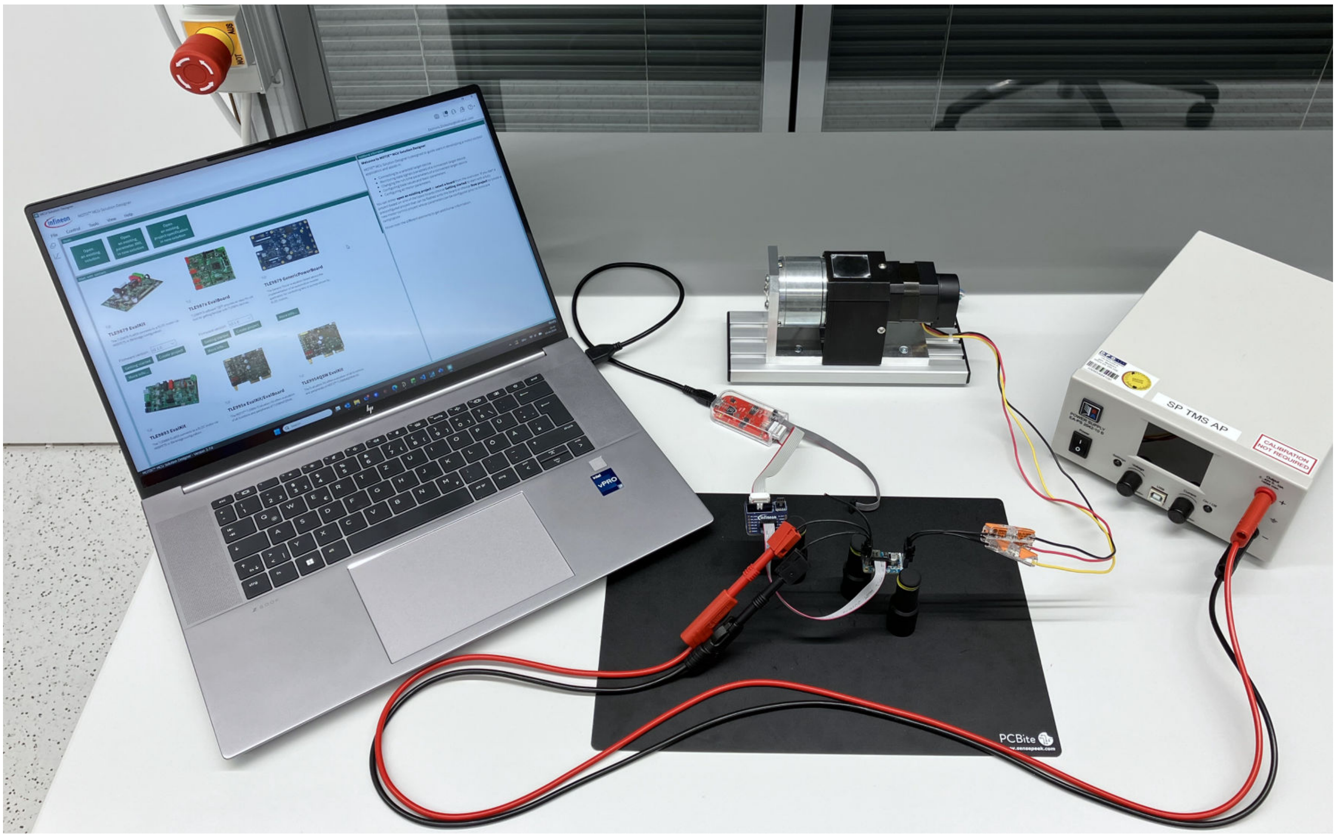

Figure 20 **Assembly picture of connected board**

Connecting the PCB for flashing and debugging only

For general debugging purposes, the 12-pin Tracebox connector on the reference design needs to be connected to the connector board. The debugger can then be connected to the 10-pin SWD connector on the connector board, allowing the use of any Arm® debugger, such as XMC™ Link, Segger J-Link, or Arm® U-Link.

In this use case, the connector board can be utilized to access some *GPIO*s of the TLE9954QSW40-33, for example, to connect external sensors.

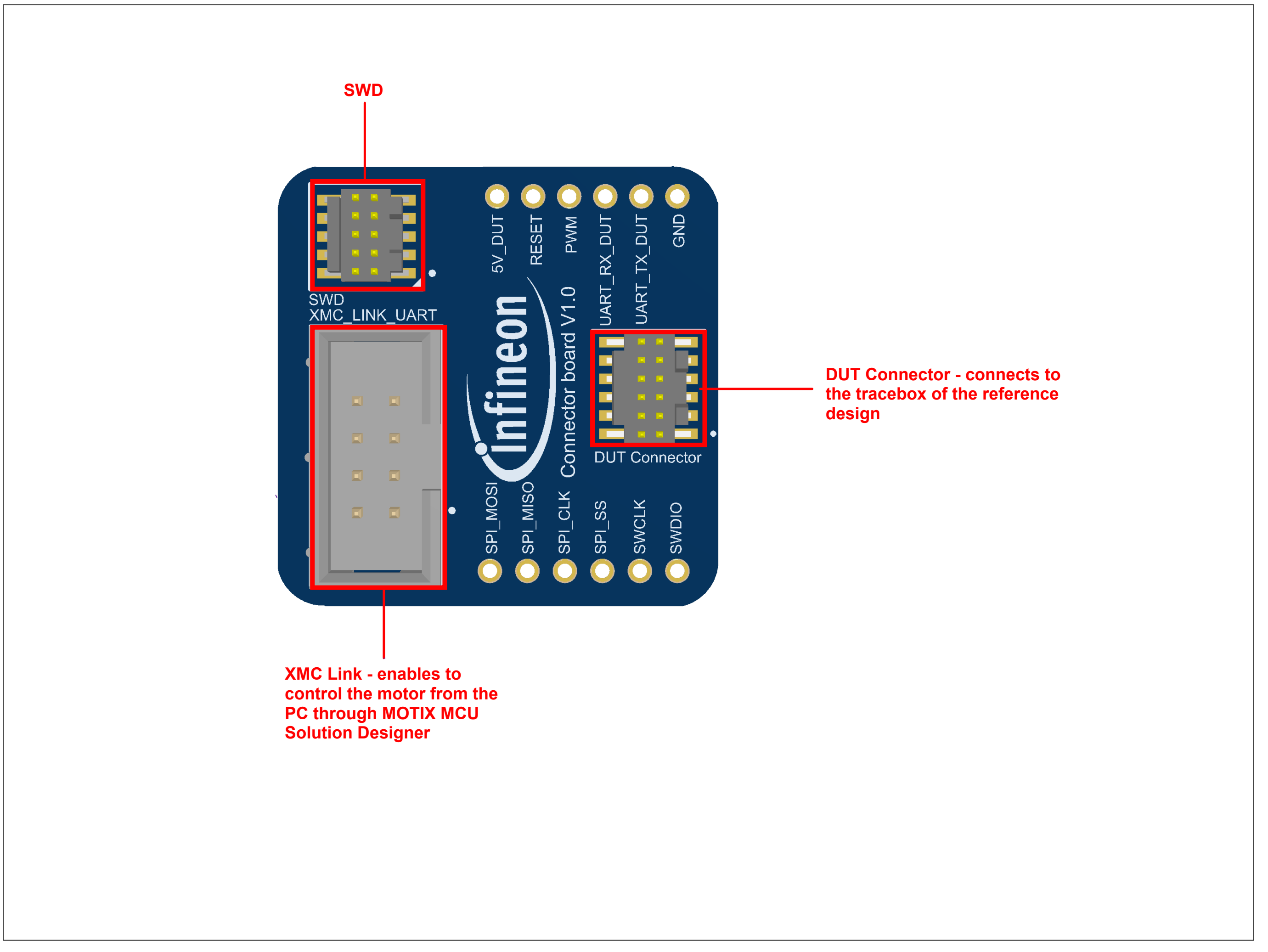

Figure 21 **Connector board**

7 System performance

The reference design showcases the performance that can be achieved with the TLE9954QSW40-33 SiP device in a highly compact *PCB* design. The following sections provide a detailed overview of the performance of the reference design, including the test setup, electrical behavior, *EMC* performance, and thermal performance, highlighting the capabilities of this compact design.

7.1 System test setup

The tests were conducted using two different setups: either a water pump attached to an emulated water circuit with a water tank, or a simple *BLDC motor* connected to a hysteresis brake. All tests, including the setup, conditions, and results are described in the following chapters. Unless otherwise specified, the default test configuration is assumed to be as follows:

- Electrical power = ~ 100 W
- Battery voltage = 13.5 V
- Nominal speed (Waterpump) = ~4700 rpm
- Nominal speed (Nanotec DB59C024035R-A motor) = 2000 rpm

Water pump setup

The reference design, REF_MINI_CMFRT_SiP, drives an automotive *BLDC* water pump. The pump is directly connected to a system constituting of different tubes and an expansion tank to ensure that the system is free of air. Water is filled in the system to emulate the load of an automotive thermal management water cycle. The *PCB* is mounted directly to the metal body of the pump as shown in Figure 23. The load is controlled by increasing or decreasing the rotational speed of the pump.

This setup was primarily utilized for *EMC* tests, as the water tank setup provides a quieter environment compared to the hysteresis brake, allowing for a more accurate assessment of the REF_MINI_CMFRT_SiP and motor's EMC behavior without potential noise interference.

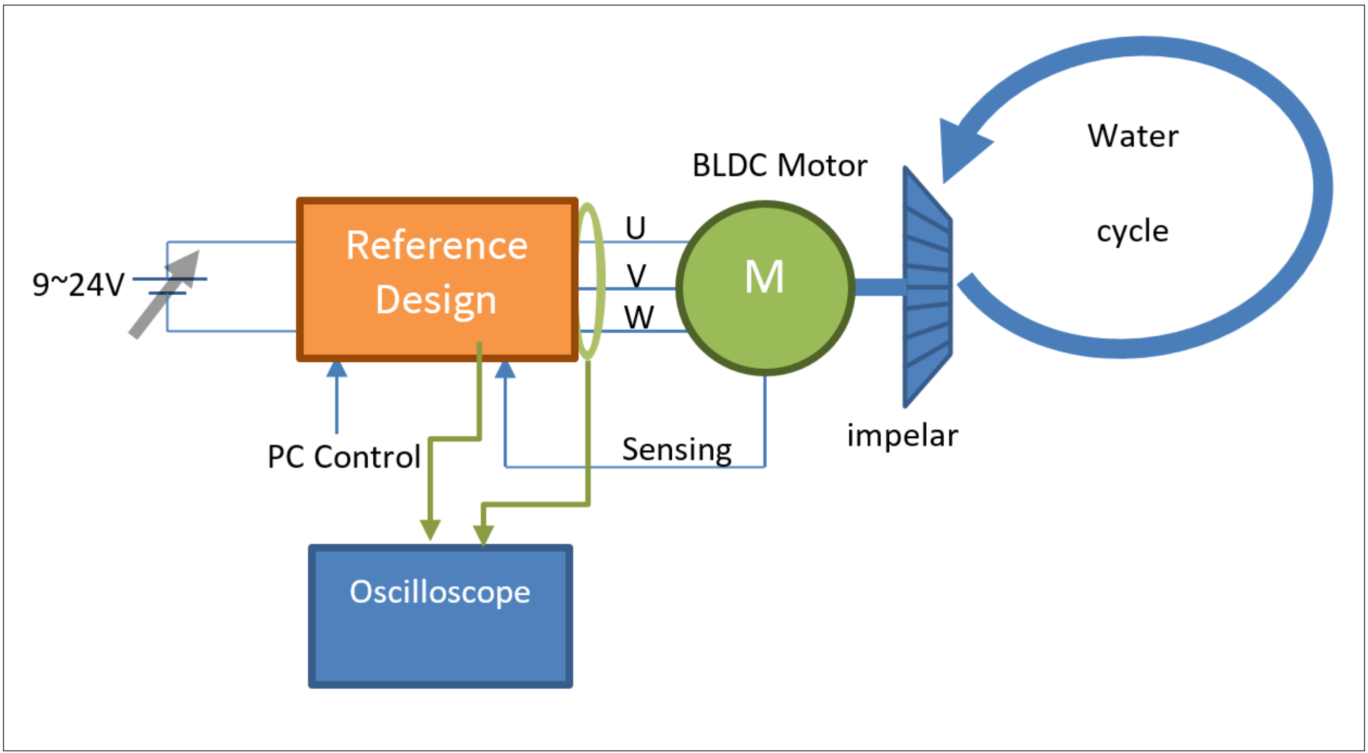

Figure 22 **Water pump test setup block diagram**

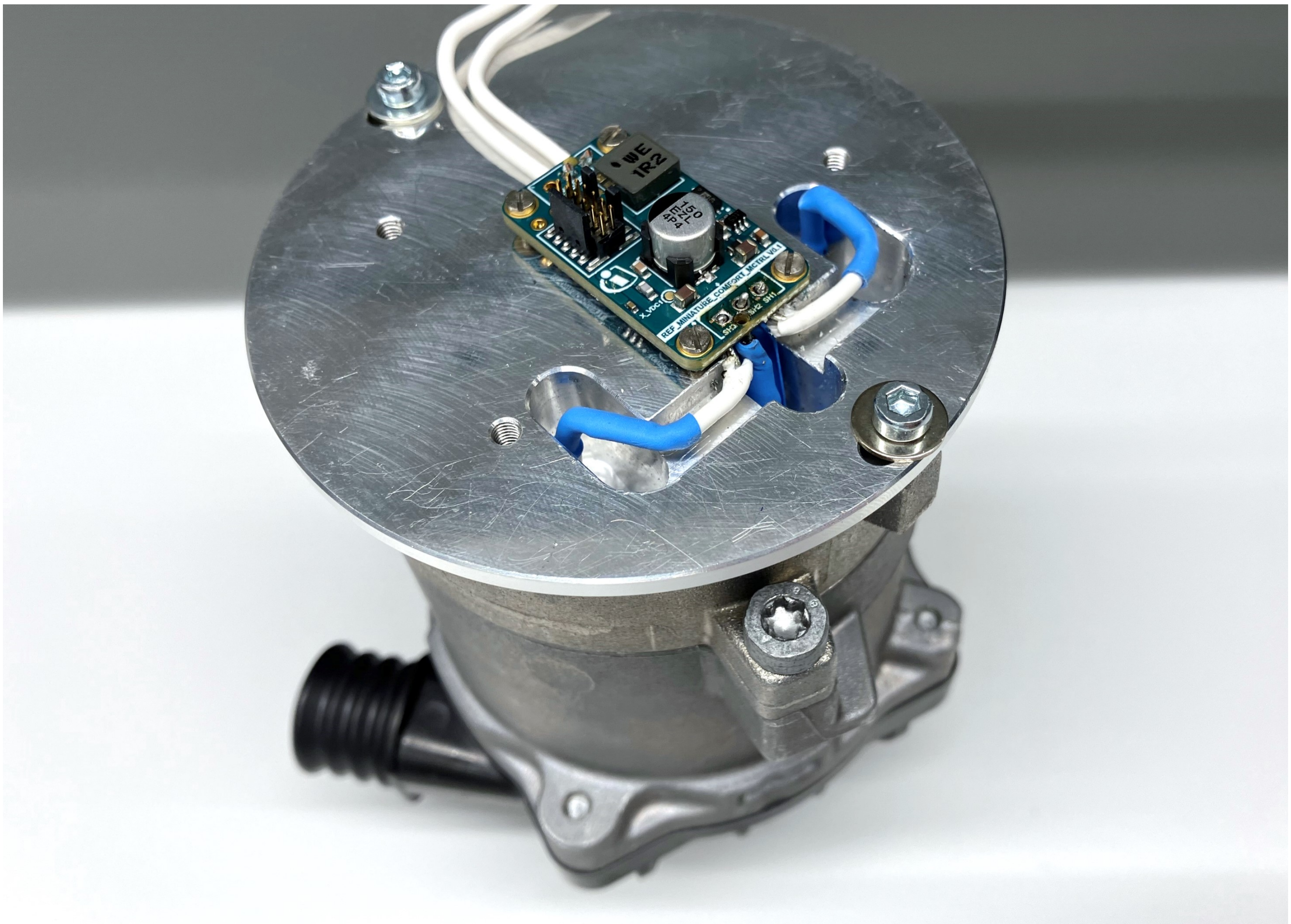

Figure 23 Assembly of PCB mounted on water pump

Hysteresis brake setup

On the second setup, the PCB is connected to the Nanotec DB59C024035R-A motor via cables. This way, different cooling conditions can be realized with and without heat sinks. The shaft of the pump is connected to a hysteresis brake via a coupling. The load to the motor can be controlled via the current into the hysteresis brake while keeping the rotational speed at around 2000 rpm.

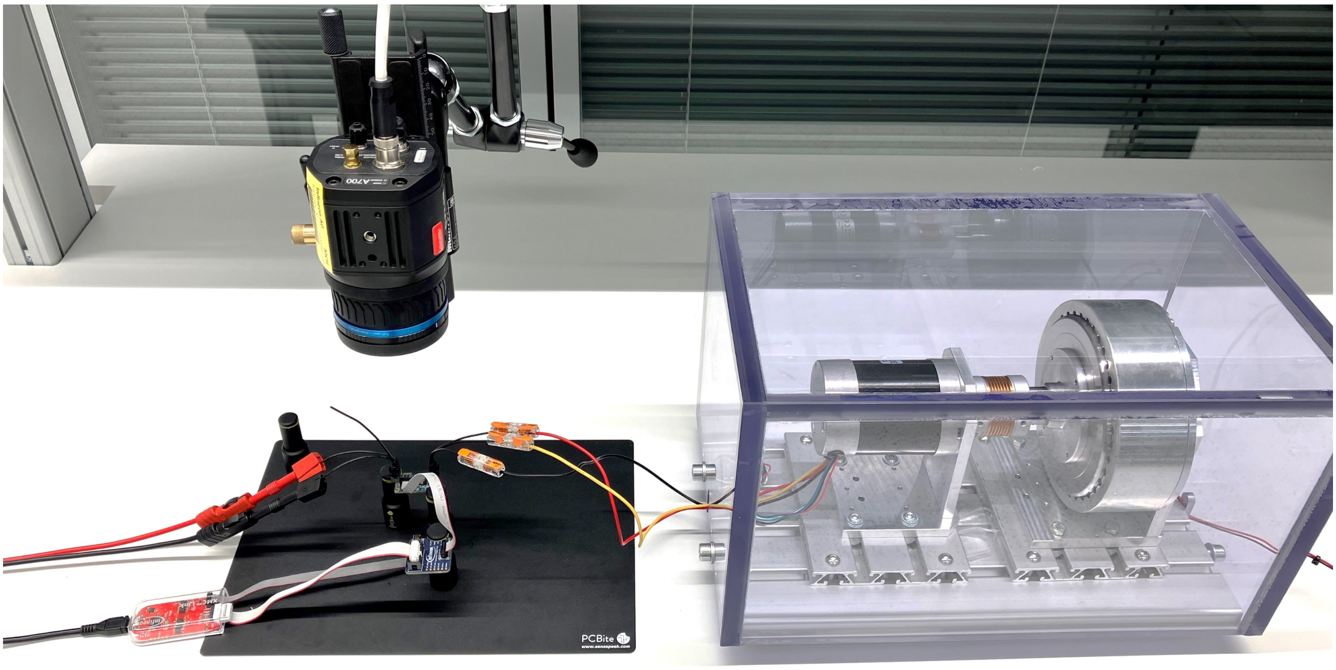

Figure 24 Picture of DB59C024035R-A and hysteresis brake setup

7.2 Electrical test result

7.2.1 Switching characteristics

The main advantage of the TLE9954QSW40-33 device is the high integration due to all B6-MOSFETs being placed inside of the package. This way the parasitic inductance in the commutation path will be reduced significantly. A lower parasitic inductance will allow for a faster switching transition.Figure 25 illustrates the difference in typical switching time ranges between both a traditional discrete solution and the TLE9954QSW40-33 System-in-Package solution.

Typical switching times are ranging between 100 ns and 200 ns. In most cases, the target is to switch as fast as possible to reduce switching losses, to keep the dead-time as short as possible, and to acquire current readings as quickly as possible after switching. The limiting factors are the *EMC* emission and maximum ratings of the gate driver due to over- and under-swing on the output voltage. Both are mostly impacted by the parasitic inductance in the commutation path. This is the reason why it is possible to switch much faster with the TLE9954QSW40-33 device. A switching time of only 60 ns should be achievable in most applications. In some cases, it is even possible to go down to 9 ns. For further details, refer to Conducted emission with motor in on-state.

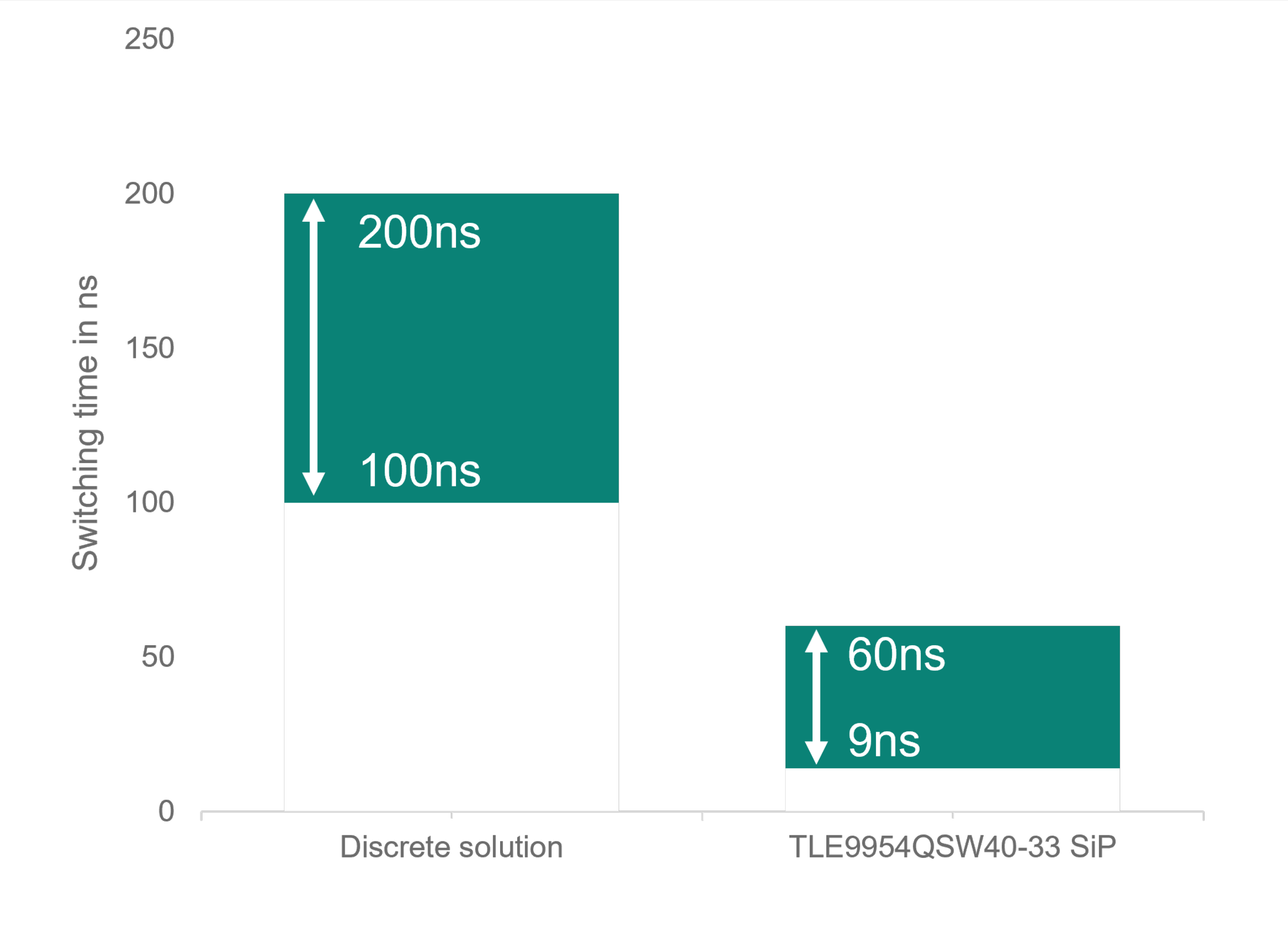

Figure 25 **Comparison of traditional switching speeds in discrete solutions vs. TLE9954QSW40-33 switching speeds**

To find the ideal switching speed, three main aspects must be considered:

- Power losses in the MOSFET during switching
- EMC emission due to switching
- Maximum rating of the device

Generally a faster switching transition is desired to reduce the power loss in the MOSFET. On the down side, faster switching leads to higher EMC emission. The EMC emission will be worse with higher parasitic inductance in the commutation path. Additionally, the combination of fast switching and parasitic inductance lead to positive and negative spikes on the outputs during the switching event. These spikes may exceed the maximum rating of the gate driver and must be avoided at all costs. In most cases, the maximum rating to look at is the maximum negative voltage at SHx. There will be a negative voltage spike at SHx during the High-Side turn-off switching event.

Figure 26 and Figure 27 show a scope capture of the high-side and low-side switching behavior of the REF_MINI_CMFRT_SIP. The gate driver was configured to maximum gate current and switching time was measured as time between 20% and 80% of SHx voltage. In the scope capture, the low-side MOSFET has a rise and fall time of 12.5 ns and 9.4 ns respectively, which is very fast. The high-side MOSFET is switching slightly slower with 18.7 ns and 16.4 ns. It can be observed in Figure 28 that the negative spike is not even exceeding the -5 V mark which is well within the maximum rating.

Switching as fast as shown in the below figures comes with the following advantages:

- Very low switching losses

- Very short dead-time possible which gives more time for phase current measurements
- Changing application conditions (voltage, current, temperature) and production spread will cause only minor deviations in switching times

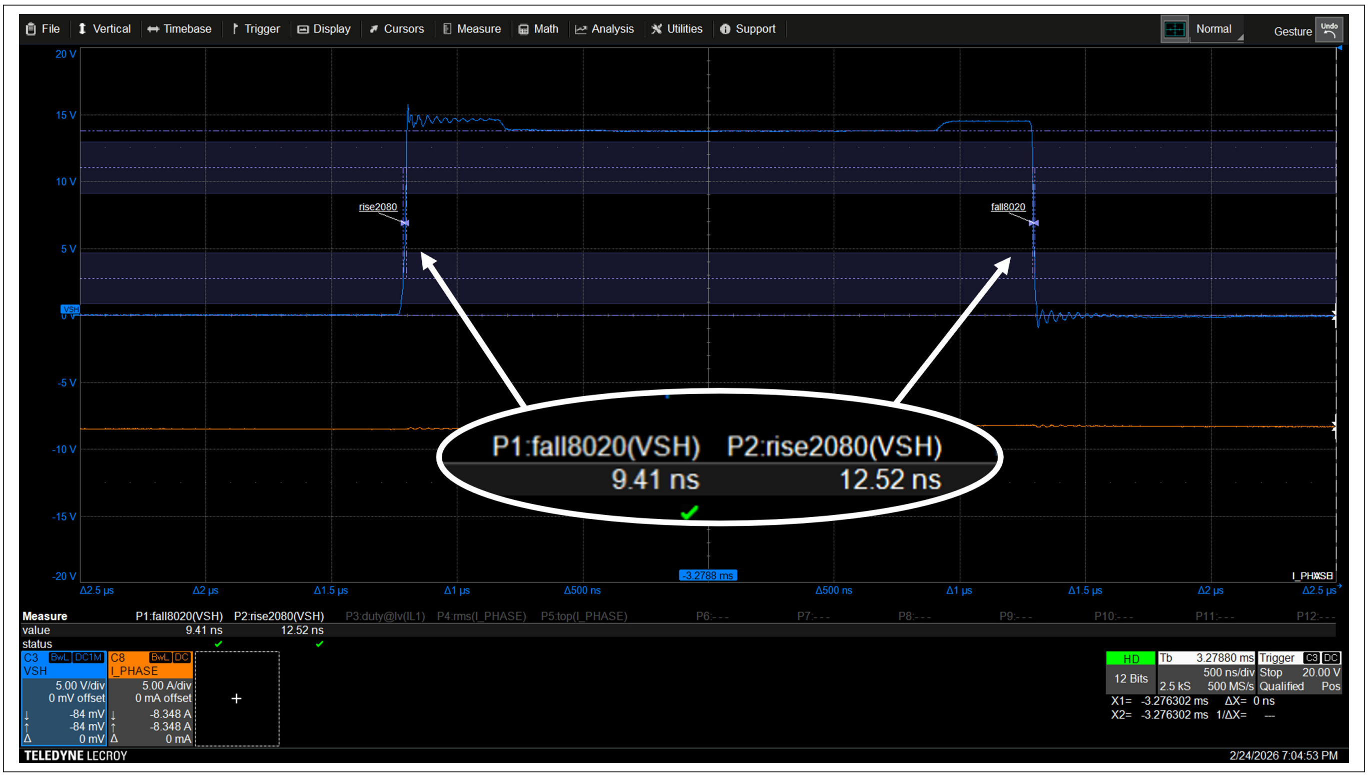

Figure 26 **Low-side switching behavior**

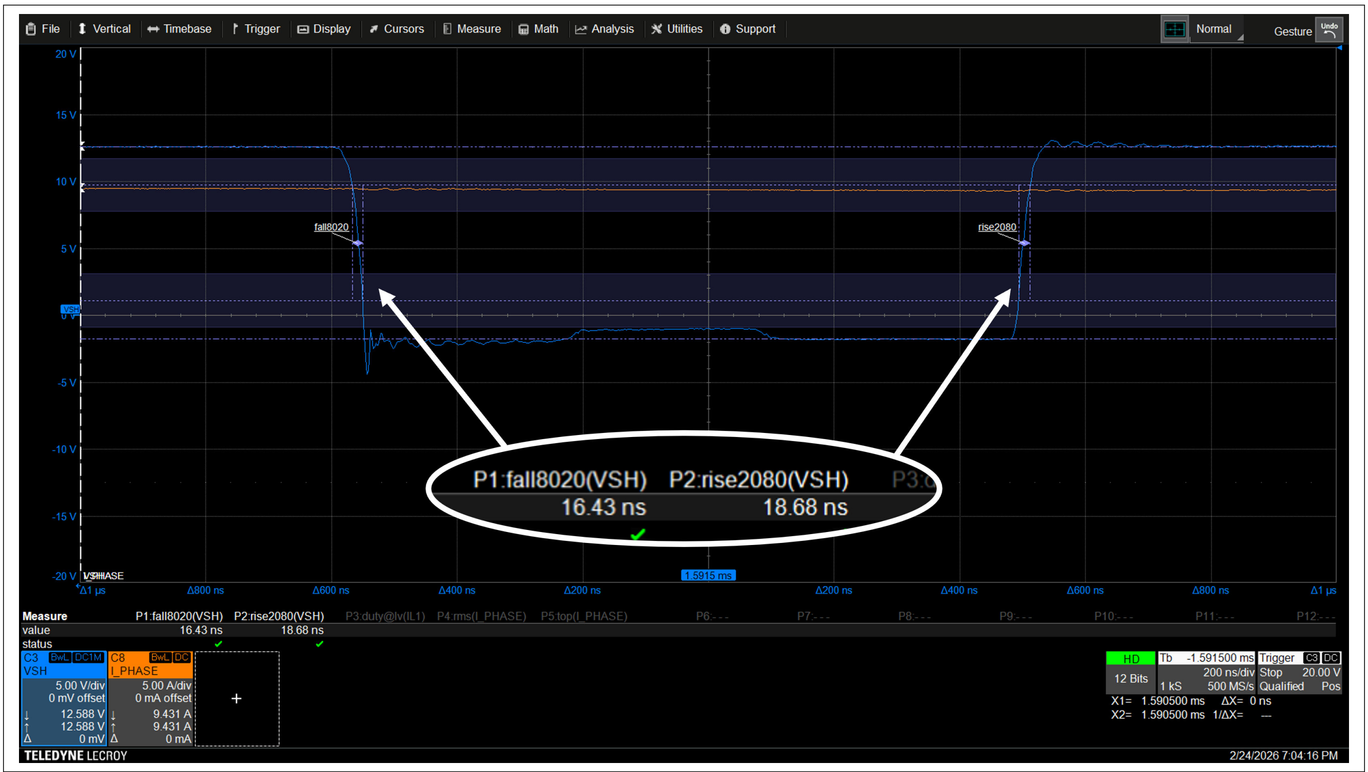

Figure 27 **High-side switching behavior**

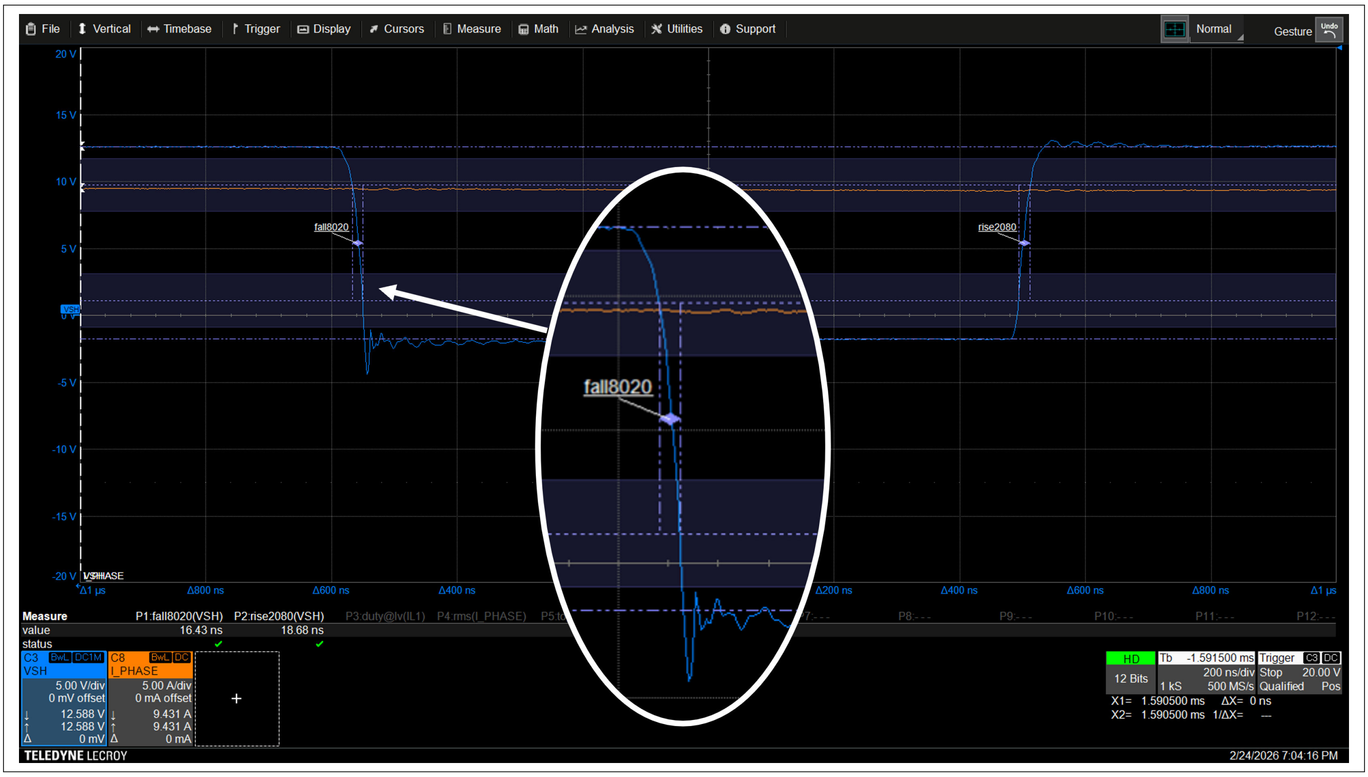

Figure 28 Negative spike during high-side turn-off

7.3 Thermal behavior

7.3.1 Main contributors to power dissipation

To ensure the thermal performance and reliability of the reference design in various application scenarios, it is crucial to understand the thermal energy dissipated by the active components. The primary contributor to self-heating is the MOSFETs integrated within the TLE9954QSW40-33 device. A well-designed thermal management system aims to minimize power dissipation and efficiently dissipate heat away from the device. Unlike traditional 3-phase motor drive *PCB*s, where shunt resistors also contribute to power dissipation, the REF_MINI_CMFRT_SIP features a XENSIV™ *TMR* sensor that measures current within the PCB, eliminating the need for a shunt resistor and resulting in reduced power losses on the board.

7.3.2 Thermal testing test setup

To assess the heat generated by the active components on the reference design, a thermal camera was employed to capture the temperature profile of the key components at an ambient temperature of 25°C. The reference design was elevated 5 cm above the desk surface using spacers to ensure unobstructed airflow. An image of the *PCB* assembled with the water pump is provided below, illustrating the setup of thePCB.

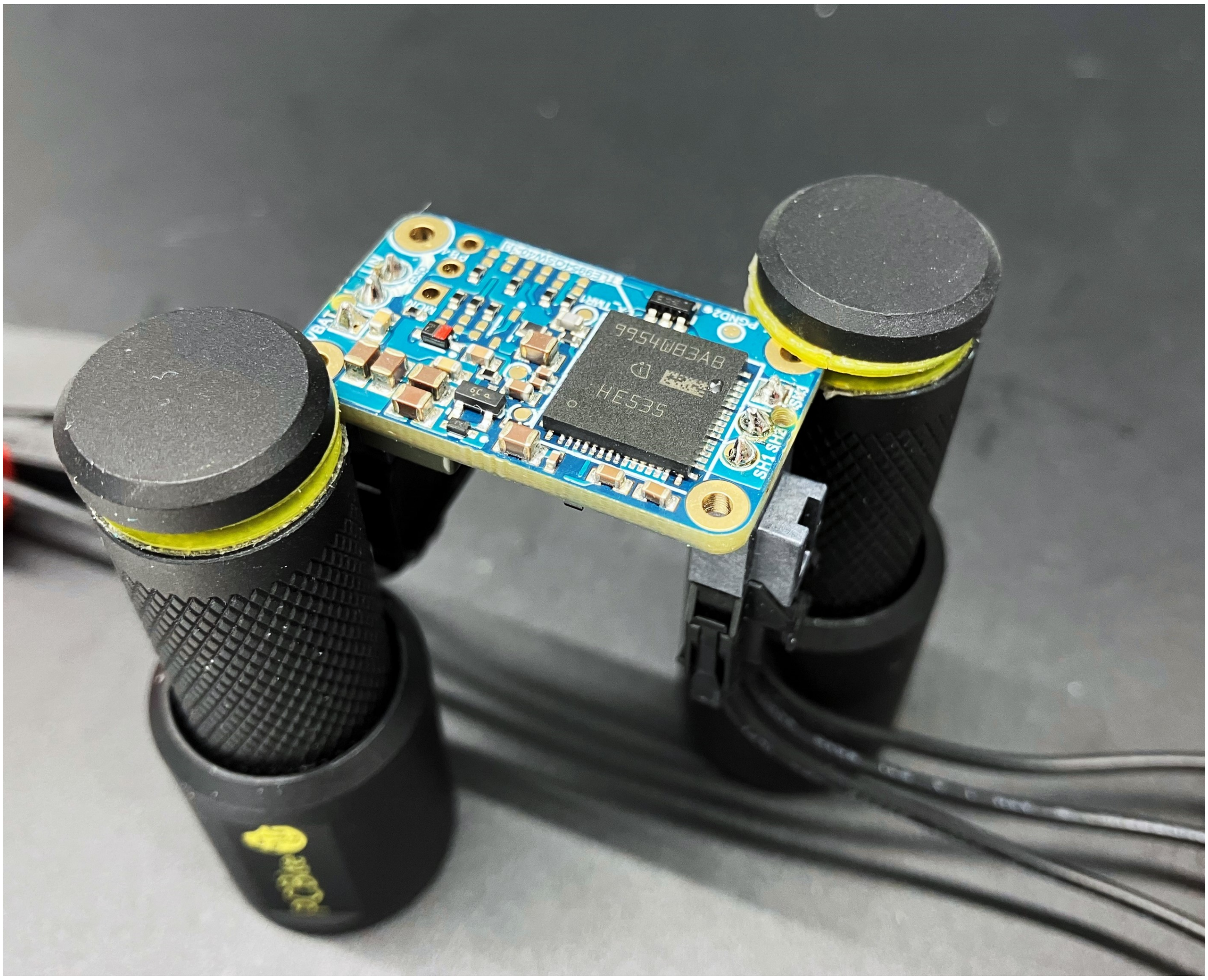

Figure 29 **Image of REF_MINI_CMFRT_SIP without heat sink and under natural convection**

Additionally to the setup without any cooling, some tests were also performed with the PCB assembled to a heat sink in natural convection. Figure 30 shows the specification of the aluminum heat sink from https://www.fischerelektronik.de/.

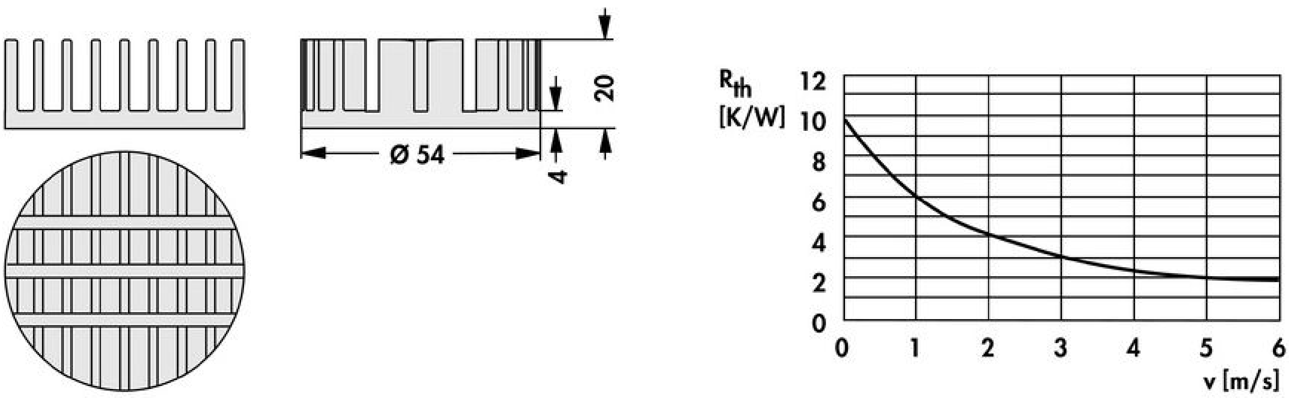

Figure 30 **Mechanical specification of aluminum heat sink**

Two different assembly methods using interface materials were evaluated. The first approach utilized a soft thermal interface pad, which was placed between the PCB and the heat sink. This setup made contact only with the components on the top of the PCB that were approximately 1.4 mm high, specifically the TLE9954QSW40-33 and certain passive components in 0804 packages. The thermal pad also served as an electrical isolator.

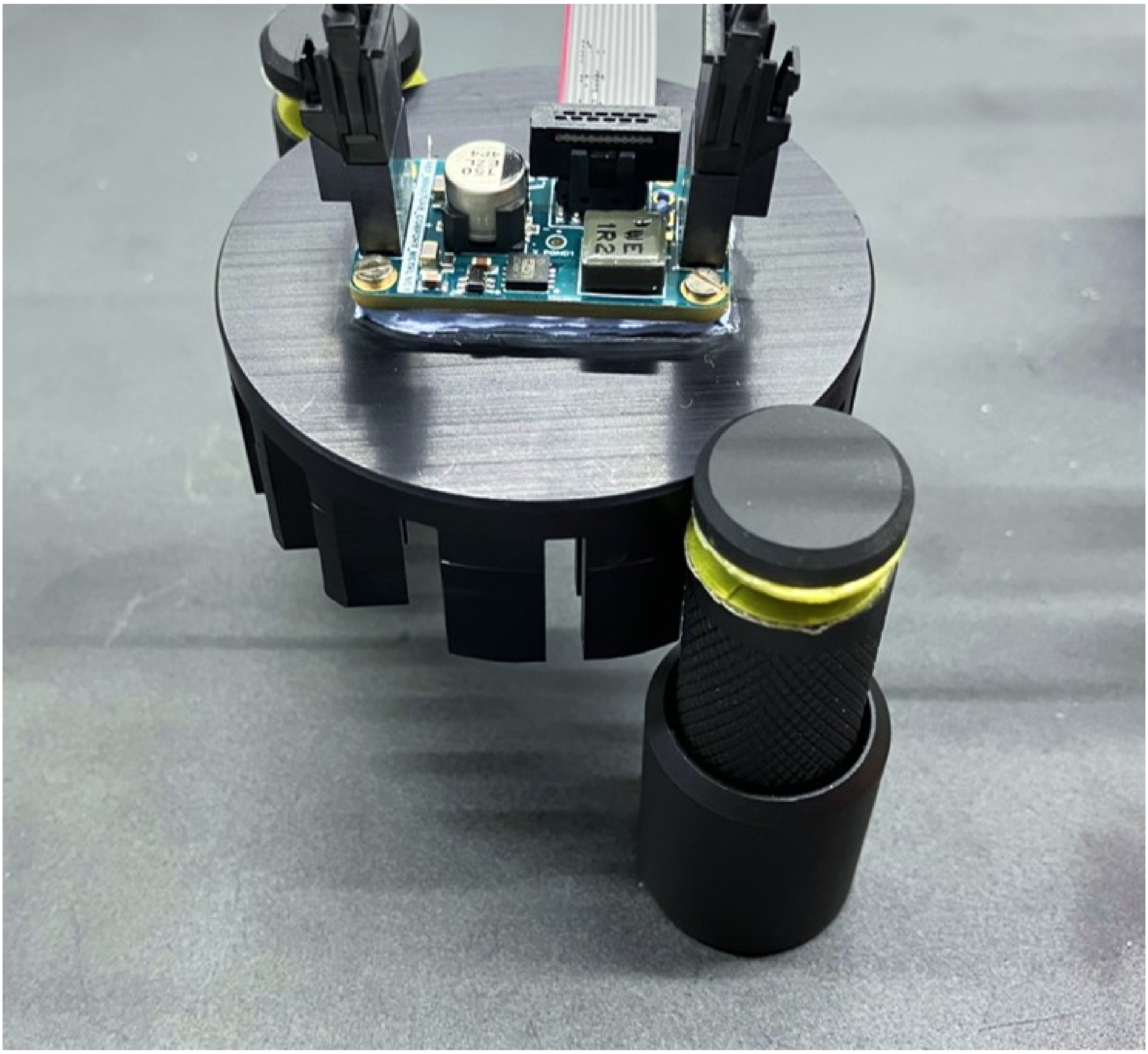

Figure 31 **Picture of assembly on heat sink using thermal interface gap filler**

In the second setup, a gap filler was used as the thermal interface material. The gap filler made contact with all components on the top side of the PCB, as well as the PCB's surface area itself. To ensure electrical isolation between the electrical components and the metal heat sink, 0.254 mm thick spacers were incorporated into the gap filler. The specific gap filler used was the Bergquist Gap Filler TGF 4000 from Henkel. The figure below illustrates both assembly variants.

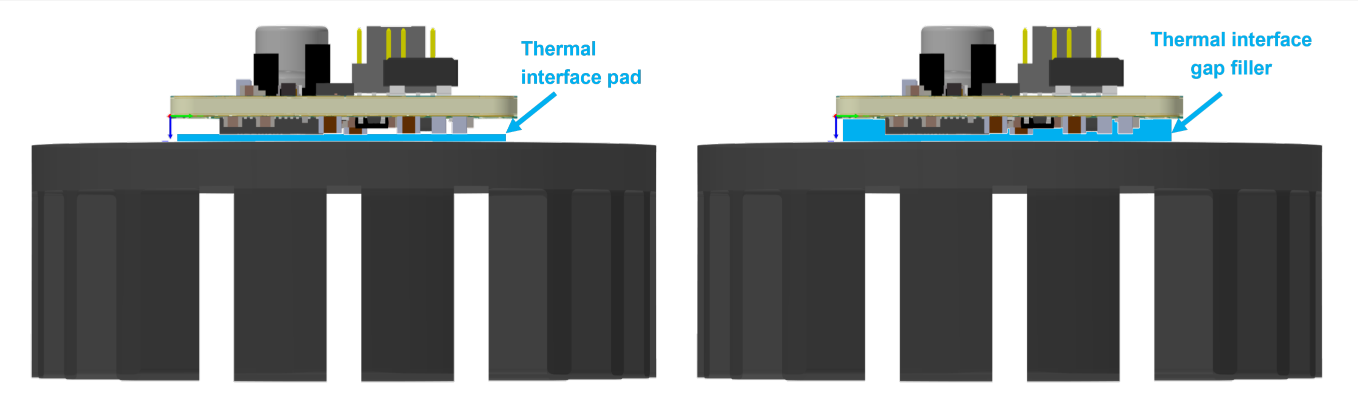

Figure 32 **Comparison of assembly on heat sink using thermal interface pad (left) and gap filler (right)**

7.3.3 Thermal analysis results

Temperature measurement on a PCB

The temperatures on the REF_MINI_CMFRT_SIP reference design were measured using an infrared camera in two different setups. Figure 33 shows the *PCB* in natural convection without a heat sink, with the IR camera capturing the top side of the PCB. The temperature readings are provided for the TLE9954QSW40-33, *TMR* sensor, and PT100 temperature sensor, giving an indication of the thermal distribution on the PCB. In contrast, Figure 34 depicts the PCB in natural convection with a heat sink, where the TLE9954QSW40-33 is facing the heat sink and a thermal interface pad is used as the thermal interface material. Since the top side of the PCB is attached to the heat sink, the IR camera shows the bottom side of the PCB, with temperature readings provided for the PI-Filter Coil, Charge Pump diodes, surface of the heat sink, copper plane below the PCB sensor, and copper plane below the VDC of the TLE9954QSW40-33. Both figures represent the steady-state condition at a 100 W load. It is noted that the infrared camera readings cannot be directly compared between the two setups due to the different configurations. To enable comparison, a PT100 temperature sensor was glued onto the SL polygon, right next to the SL output of the TLE9954QSW40-33, and its readings are used for evaluating the impact of different cooling concepts, as shown in Figure 36.

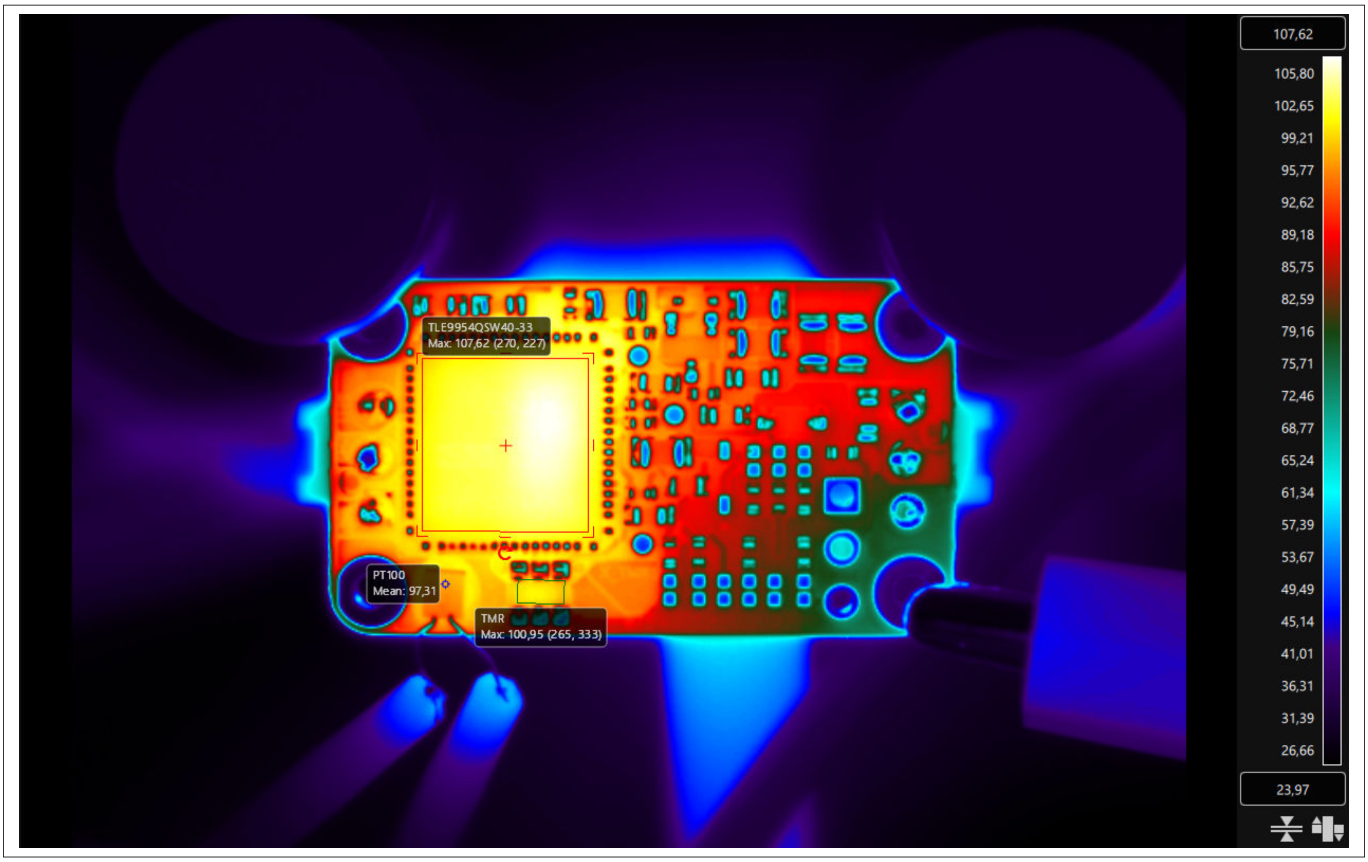

Figure 33 IR-camera recording of temperature distribution on PCB at 100 W without heat sink

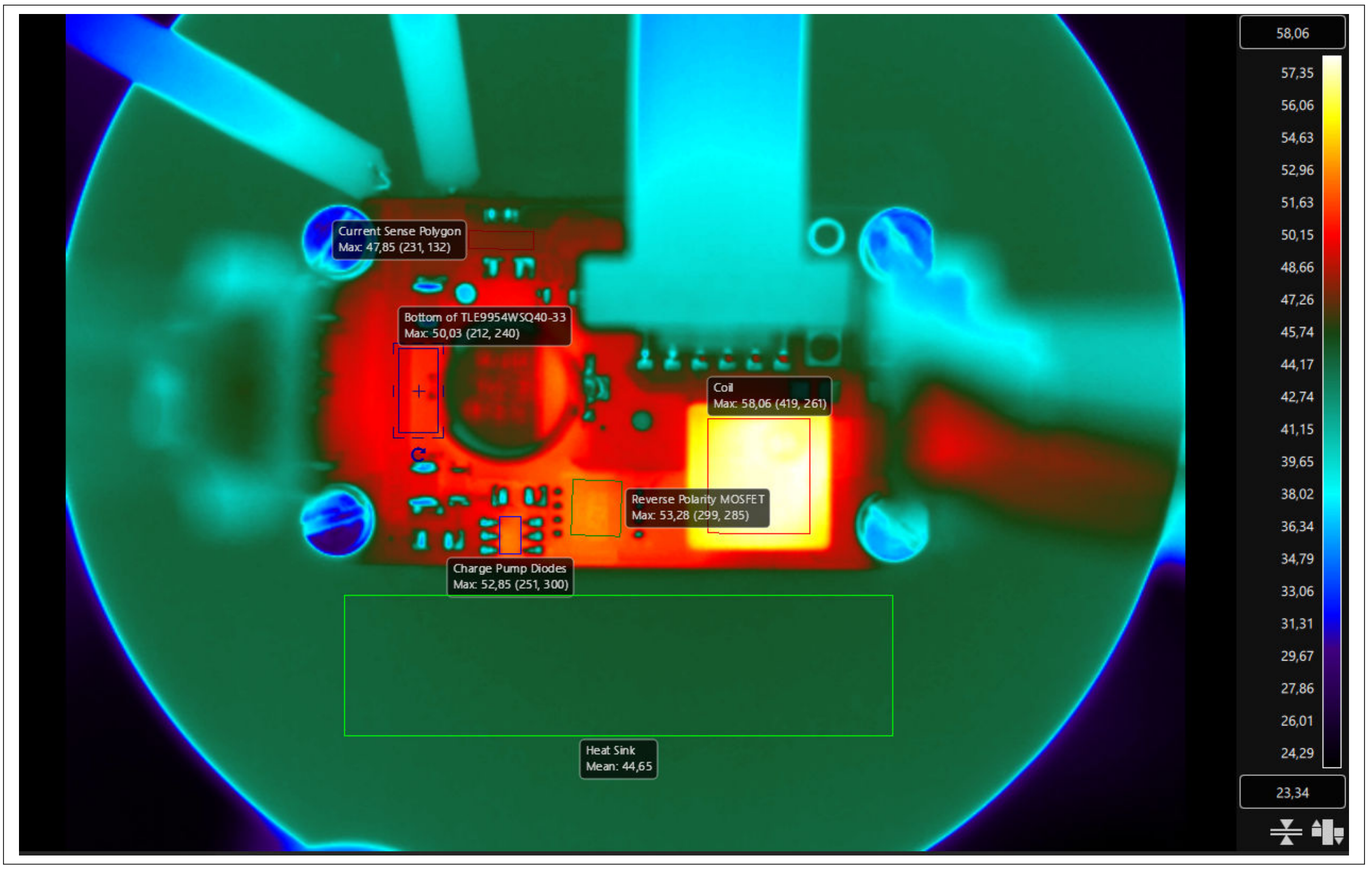

Figure 34 **IR-camera recording of temperature distribution on PCB at 100 W with heat sink and thermal interface pad**

Heating curve of the device

Figure 35 illustrates the thermal behavior of the TLE9954QSW40-33, with the higher temperature curve (red) representing the maximum temperatures and the lower temperature curve (red) representing the average temperatures. This plot shows the heating curves over a period of approximately 11 minutes, depicting how the temperatures rise and eventually settle over time, reaching a steady-state condition.

The following section presents a comparison of various cooling concepts, with all test results expressed as delta temperatures relative to the ambient temperature.

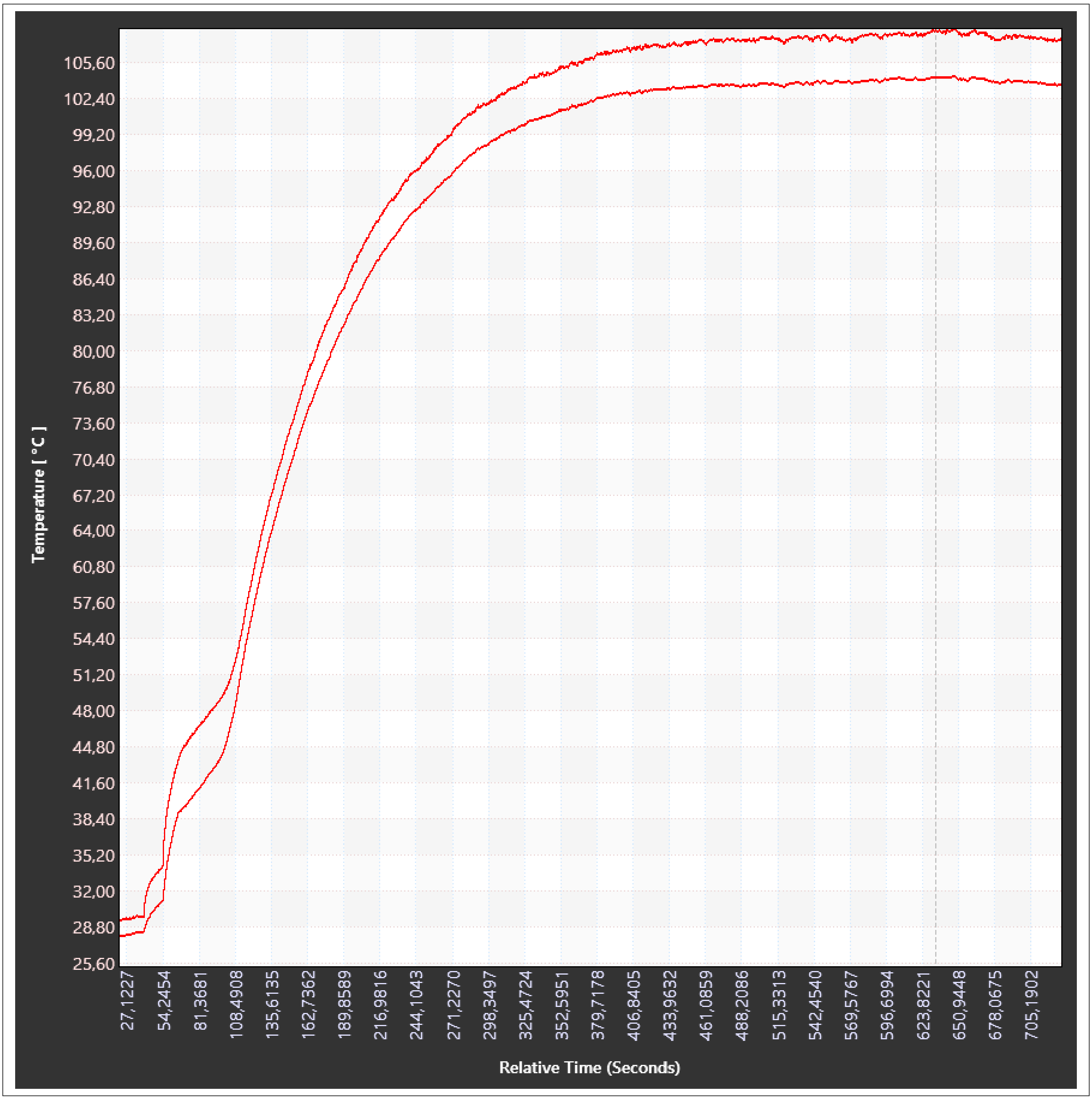

Figure 35 **Plot of maximum (top) and mean (bottom) temperatures on TLE9954QSW40-33 over time without heat sink**

Comparison of different cooling concepts

Figure 36 presents a comparison of different cooling concepts, illustrating the delta temperature (ΔT) at steady state after continuously driving the motor for up to 30 minutes at power levels of 50 W, 100 W, and 120 W, respectively. Notably, all tests were conducted using the fast switching configuration.

The green bars represent the setup without a heat sink, the gray bars represent the setup with a heat sink and a thermal interface pad, and the orange bars represent the setup with a heat sink and a thermal interface gap filler.

Temperature rise increases with output power for all configurations, but the increase is steepest without cooling. Adding a thermal interface pad substantially reduces the temperature rise, while the thermal interface gap filler provides the lowest temperature rise across the range. Overall, both interface materials significantly improve thermal performance versus no cooling, with the gap filler consistently outperforming the pad, and the benefit becomes more pronounced at higher power. These values are based on the PT100 sensor reading and therefore represent an approximate gate driver temperature which is slightly lower than the actual peak temperature within the device.

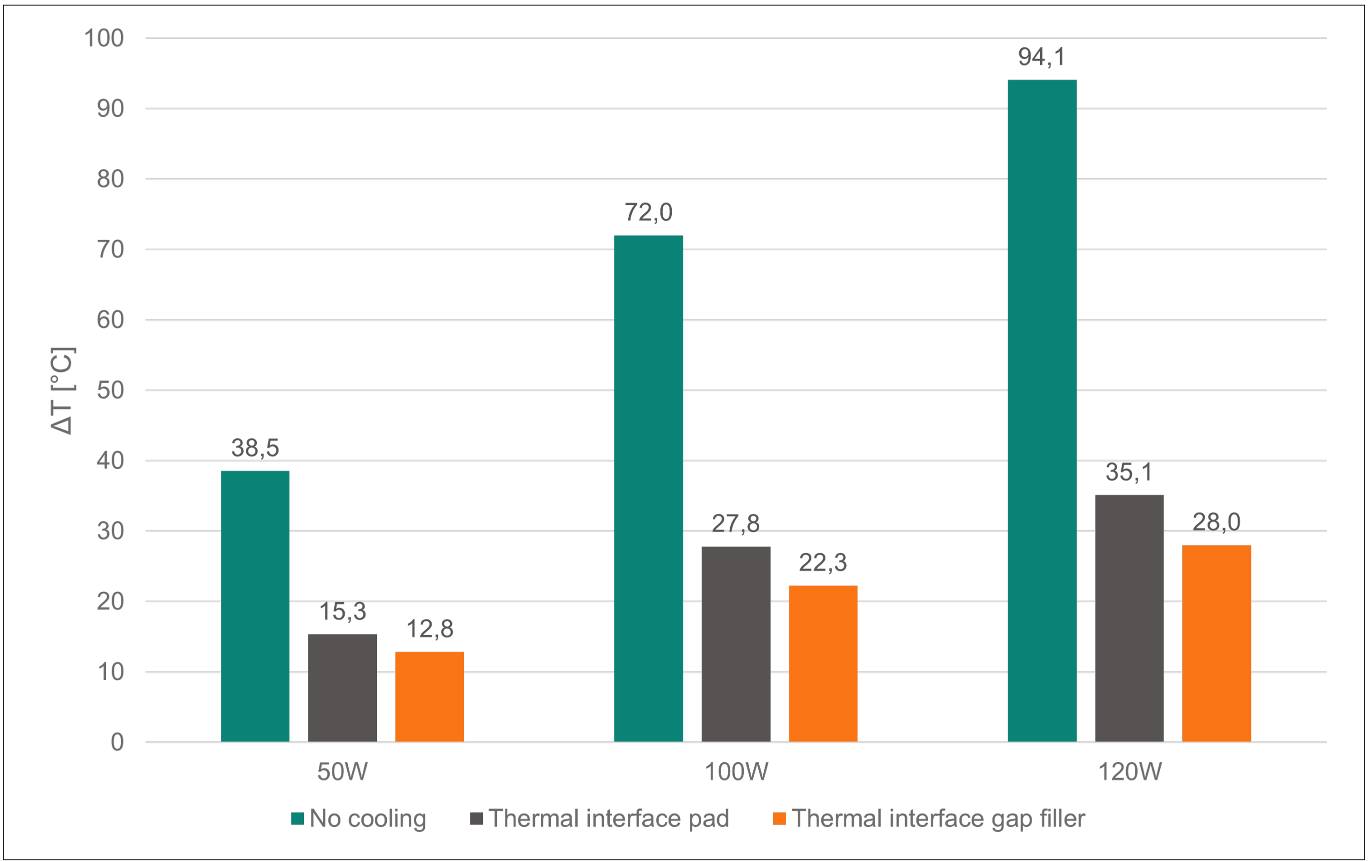

Figure 36 **Bar chart comparing different cooling concepts**

7.3.4 Thermal behavior conclusion

The thermal investigation reveals that the resulting temperature is heavily dependent on the cooling setup. Notably, the results demonstrate that cooling through the top mold compound is an effective method to enhance the power capabilities of the TLE9954QSW40-33. By implementing a strong cooling concept or operating under pulse load conditions, such as those found in 3-phase seat adjustment or power lift gate applications, it is expected that even higher power levels can be achieved.

7.4 EMC

7.4.1 EMC test setup

Figure 37 illustrates the configuration used for the *EMC* tests. On the supply side, a Line Impedance Stabilization Network (LISN) was connected to simulate the 12 V board net, and the conducted emissions on the supply lines were measured. All tests were performed under a continuous load of 100 W. Notably, one of the *PCB* mounting holes is connected to *GND*, providing a GND connection to the pump housing as well.

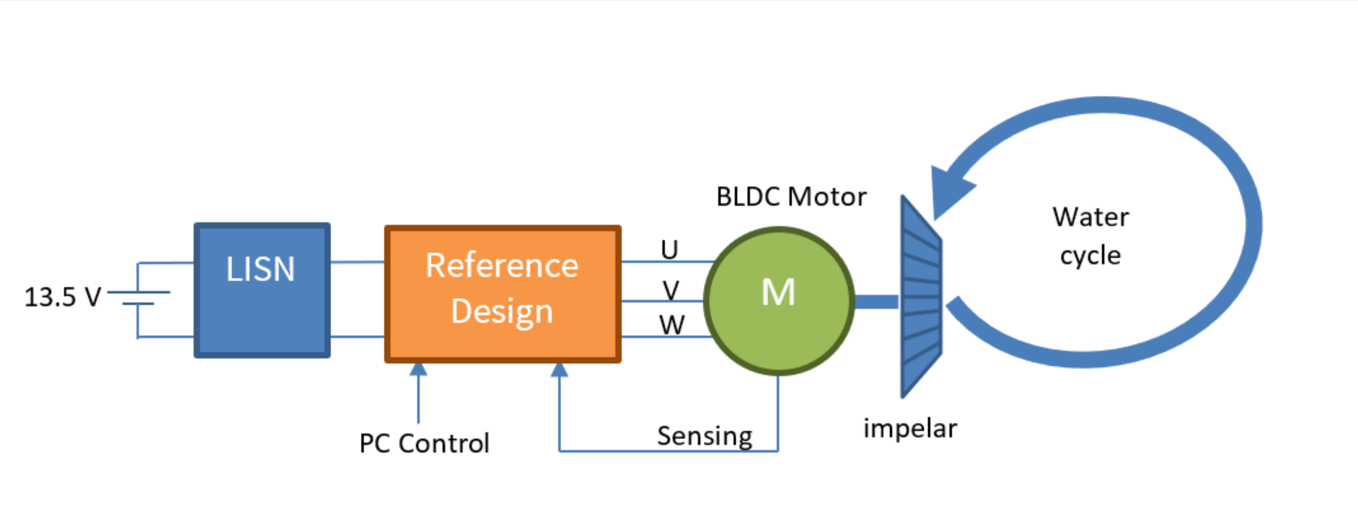

Figure 37 **Diagram of EMC test setup**

7.4.2 Conducted emission with motor in on-state

The *EMC*-conducted emission results are presented in the form of peak (Figure 38) and average (Figure 39) measurements at different switching speeds. The blue and green curves represent the emission levels for the fastest (9 ns) and medium (40 ns) switching speeds, respectively. It can be observed that at a switching speed of 9 ns, the Class 5 limits are slightly exceeded at frequencies around 100 MHz and below 200 kHz. However, reducing the switching speed to 40 ns results in a 4 dBµV decrease in the 100 MHz frequency range, bringing the measurement on the high frequency Class 5 limits. As expected, the change in switching speed has no impact on the lower frequency EMC emission. For both switching speeds, the peak measurements are well within the Class 4 limits which are not displayed in the plots.

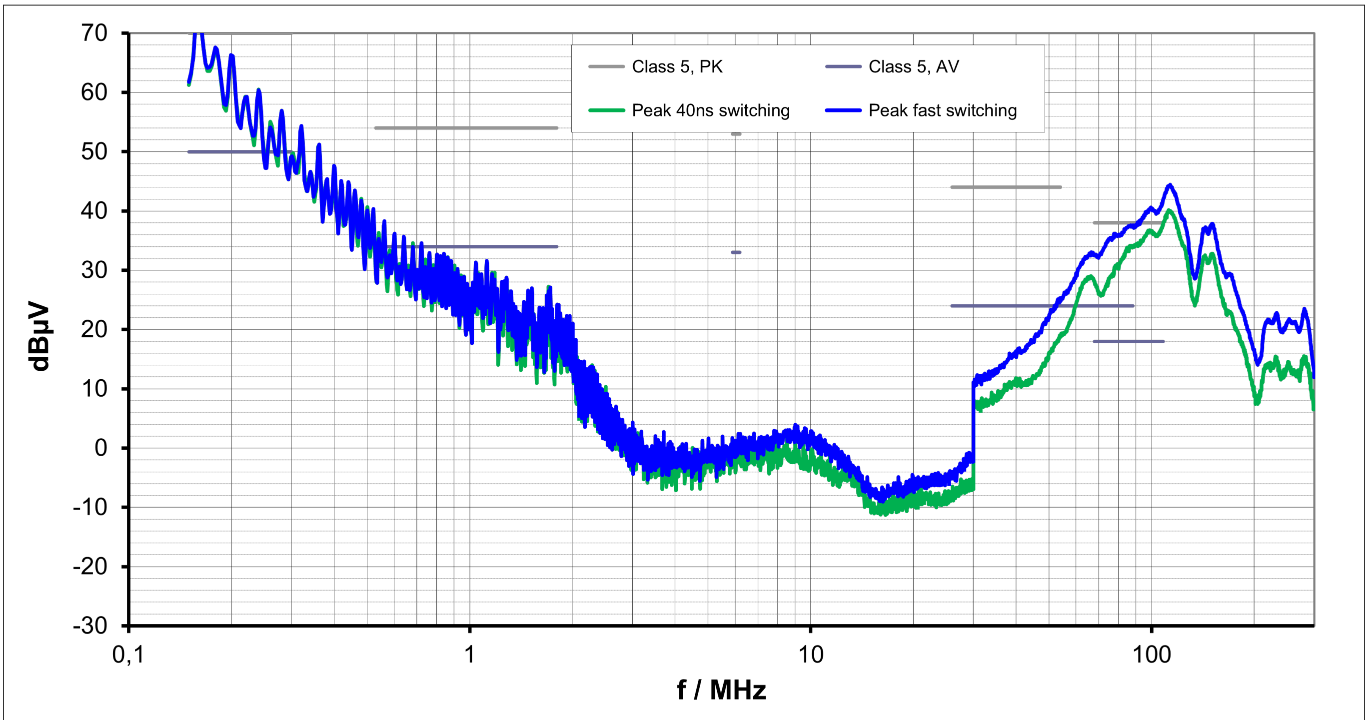

Figure 38 **EMC peak measurements at different switching speed**

The average EMC measurement results reveal a similar trend to the peak measurements, with some notable differences. In the 9 ns switching condition, the Class 5 limits are exceeded in both the high and low frequency ranges. Furthermore, the Class 4 limits are also exceeded in both frequency ranges, indicating a higher level of electromagnetic emission. In contrast, the 40 ns switching condition yields average measurements that are within the Class 5 limits in the high frequency range, but exceed both Class 5 and Class 4 limits in the low frequency range. As expected, the switching speed is found to have a significant impact only in the higher frequency range, with the lower frequency emissions remaining unaffected.

In conclusion, a switching speed of 40 ns is recommended for the REF_MINI_CMFRT_SIP reference design to achieve Class 5 compliance in the high frequency range. However, additional measures are necessary to achieve Class 5 compliance in the low frequency range, as the current design exceeds limits in this range.

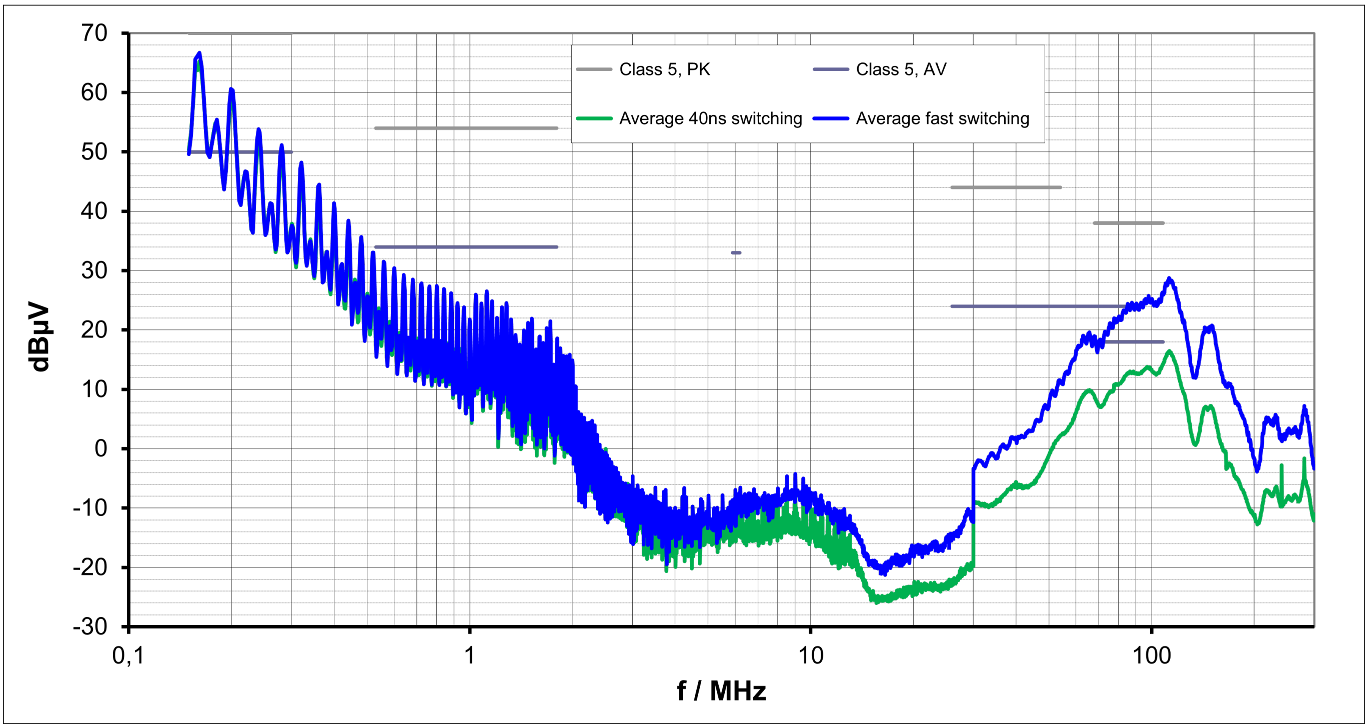

Figure 39 **EMC average measurements at different switching speed**

A second comparison to investigate the impact of modified component selection on the REF_MINI_CMFRT_SIP reference design is shown in the figures below. Specifically, the DC-Link capacitor size was increased from 150 µF to 220 µF, while maintaining the same 6 mm diameter form factor, and the PI-Filter inductance was increased from 1.2 µH to 2.2 µH, also in the same form factor. The results, shown in the plots below, reveal a significant improvement in both peak and average measurements, with a reduction of approximately 8 dBµV in the lower frequency range. This improvement is substantial, as it brings the peak measurement within the Class 5 limits for the low frequency range. Although the average measurement still exceeds Class 5 limits, it now easily meets the Class 4 requirements. These findings demonstrate that the low-frequency behavior can be massively influenced by the PI-Filter inductor and DC-Link capacitor, highlighting the importance of careful component selection.

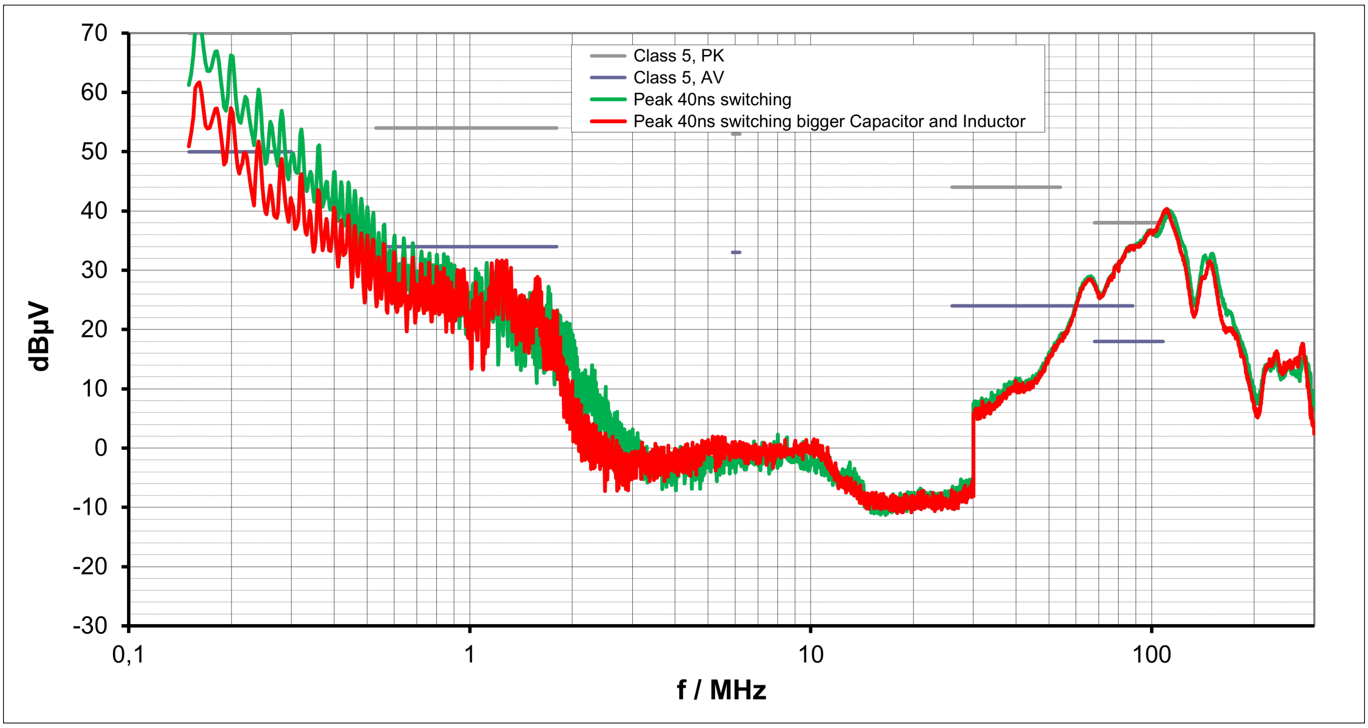

Figure 40 EMC peak measurements with 220 uF DC-Link capacitor and 2.2 uH inductor

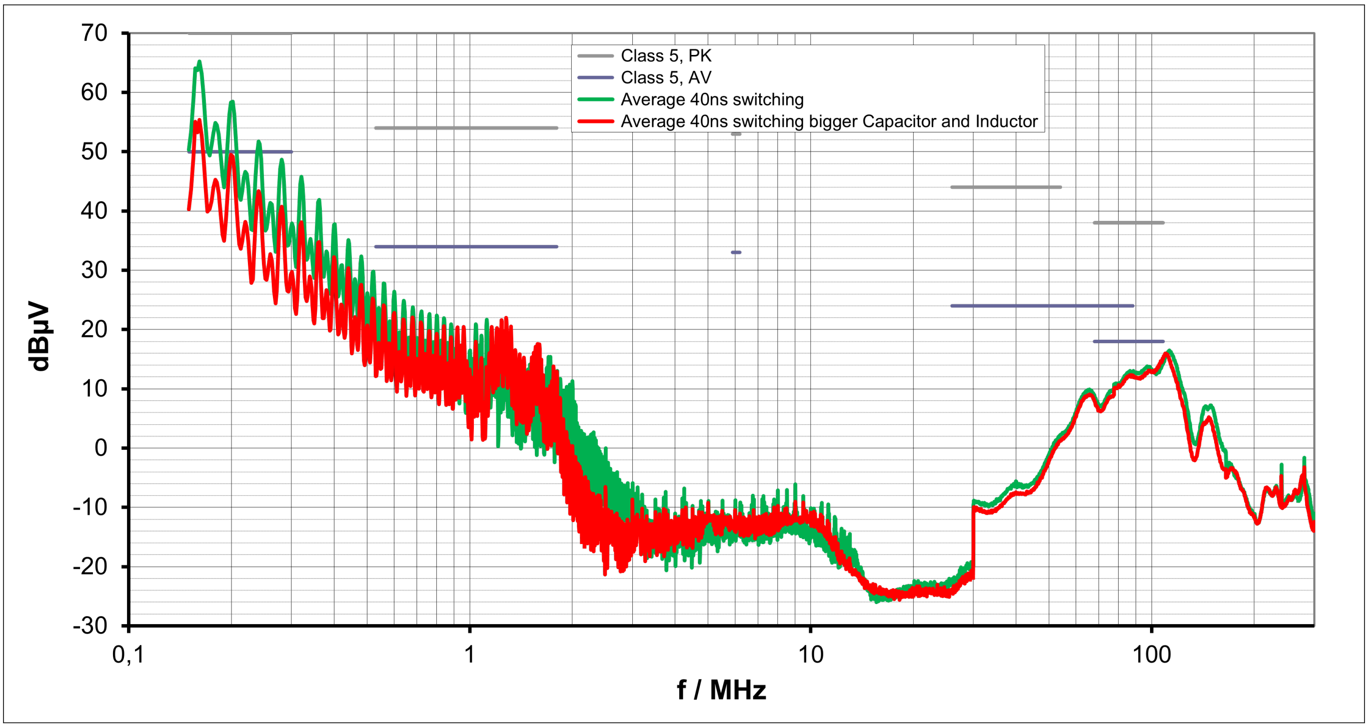

Figure 41 EMC average measurements with 220 uF DC-Link capacitor and 2.2 uH inductor

8 Project collaterals

8.1 Schematics

REF_MINI_CMFRT_SIP schematics

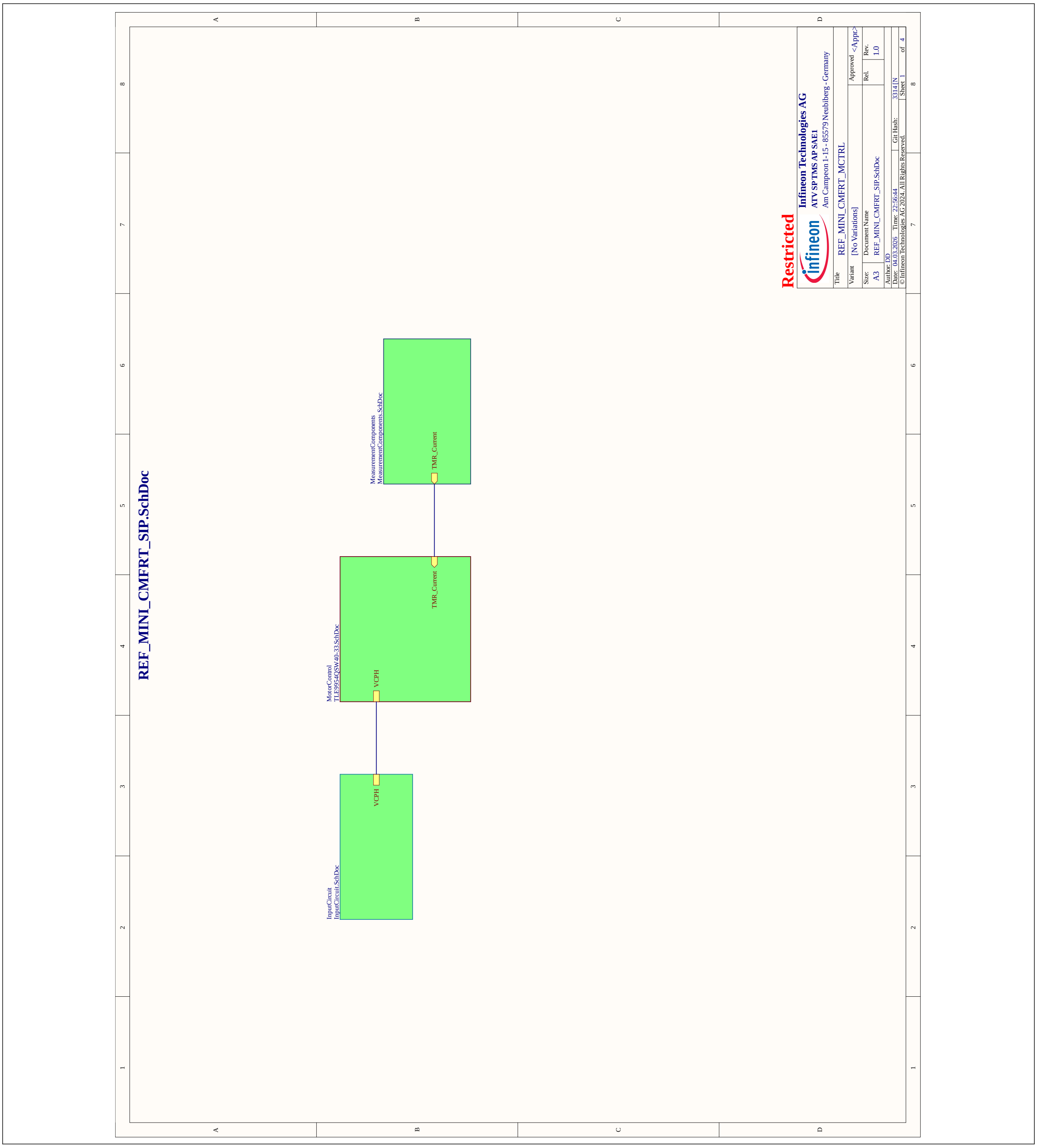

Figure 42 REF_MINI_CMFRT_SIP overview

8 Project collaterals

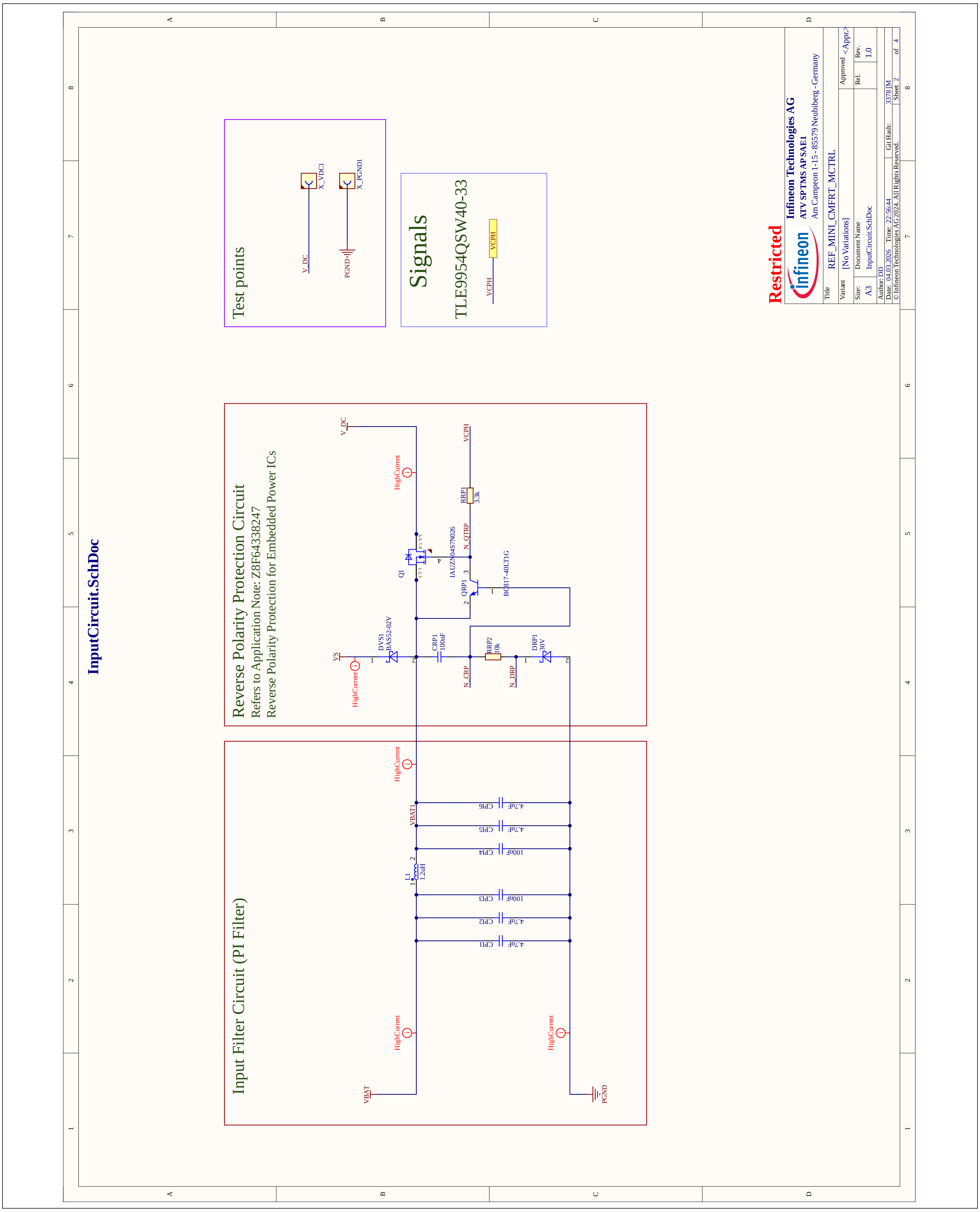

Figure 43 **Input circuit**

8 Project collaterals

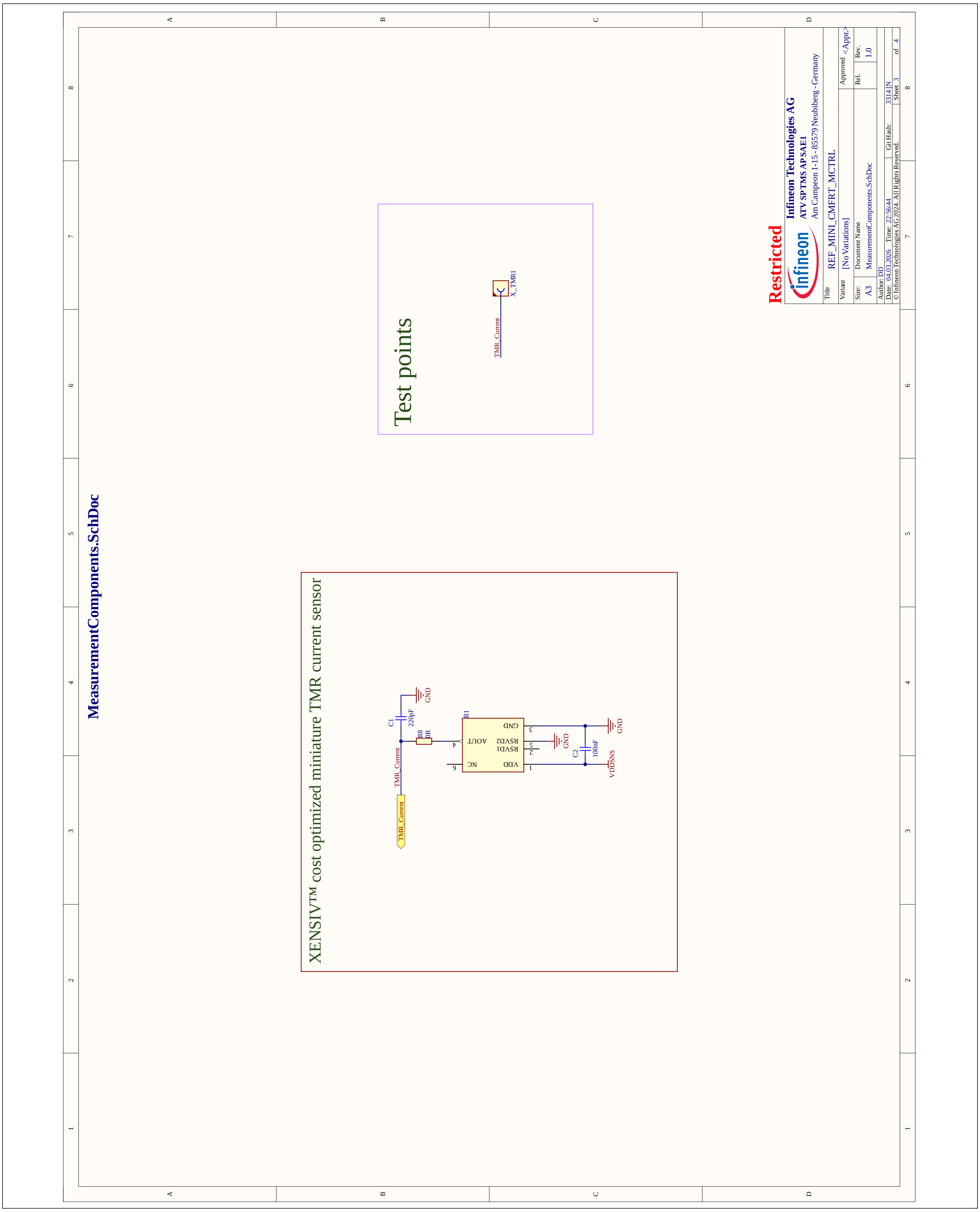

Figure 44 **Measurement components**

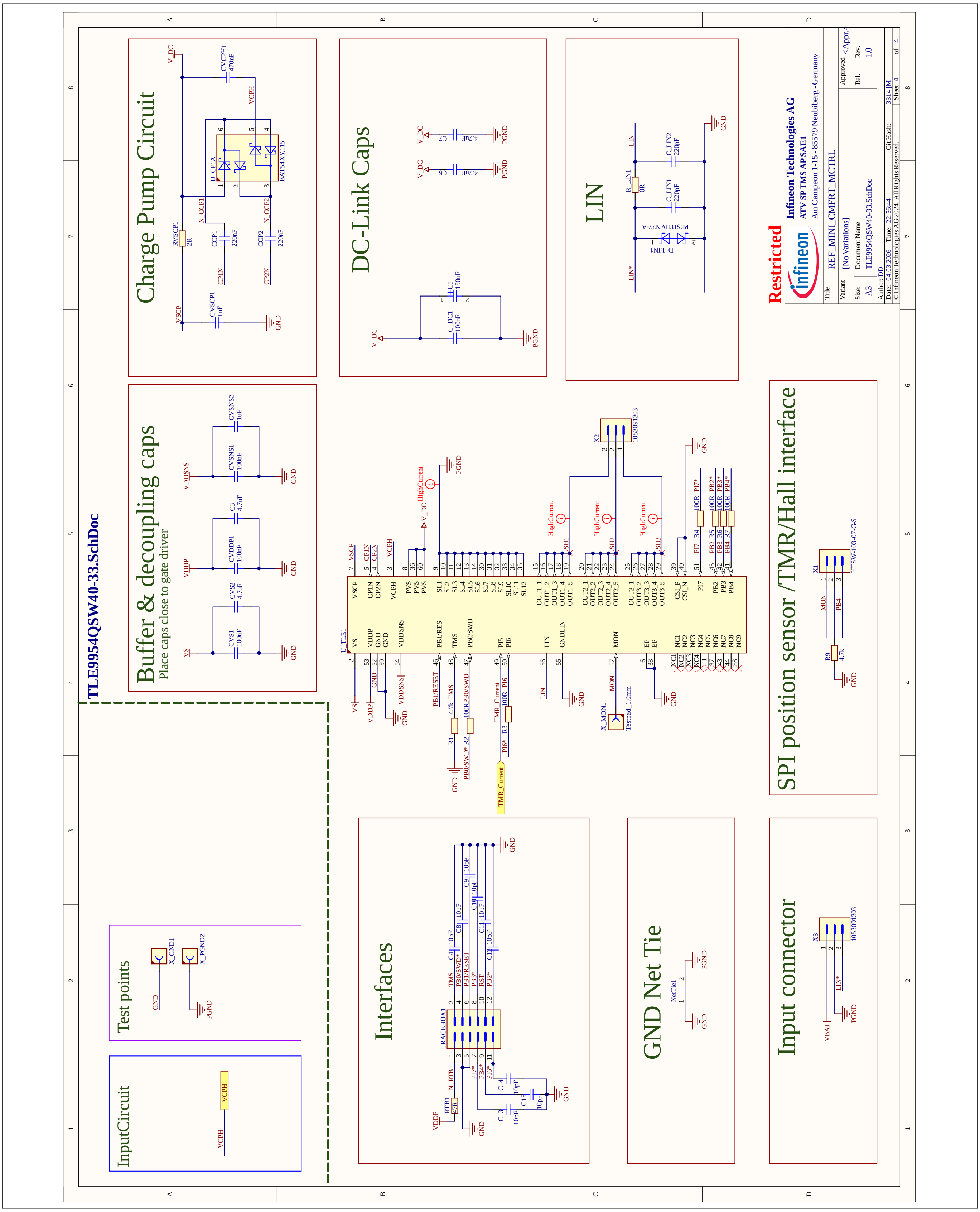

Figure 45 TLE9954QSW40-33

Connector board schematics

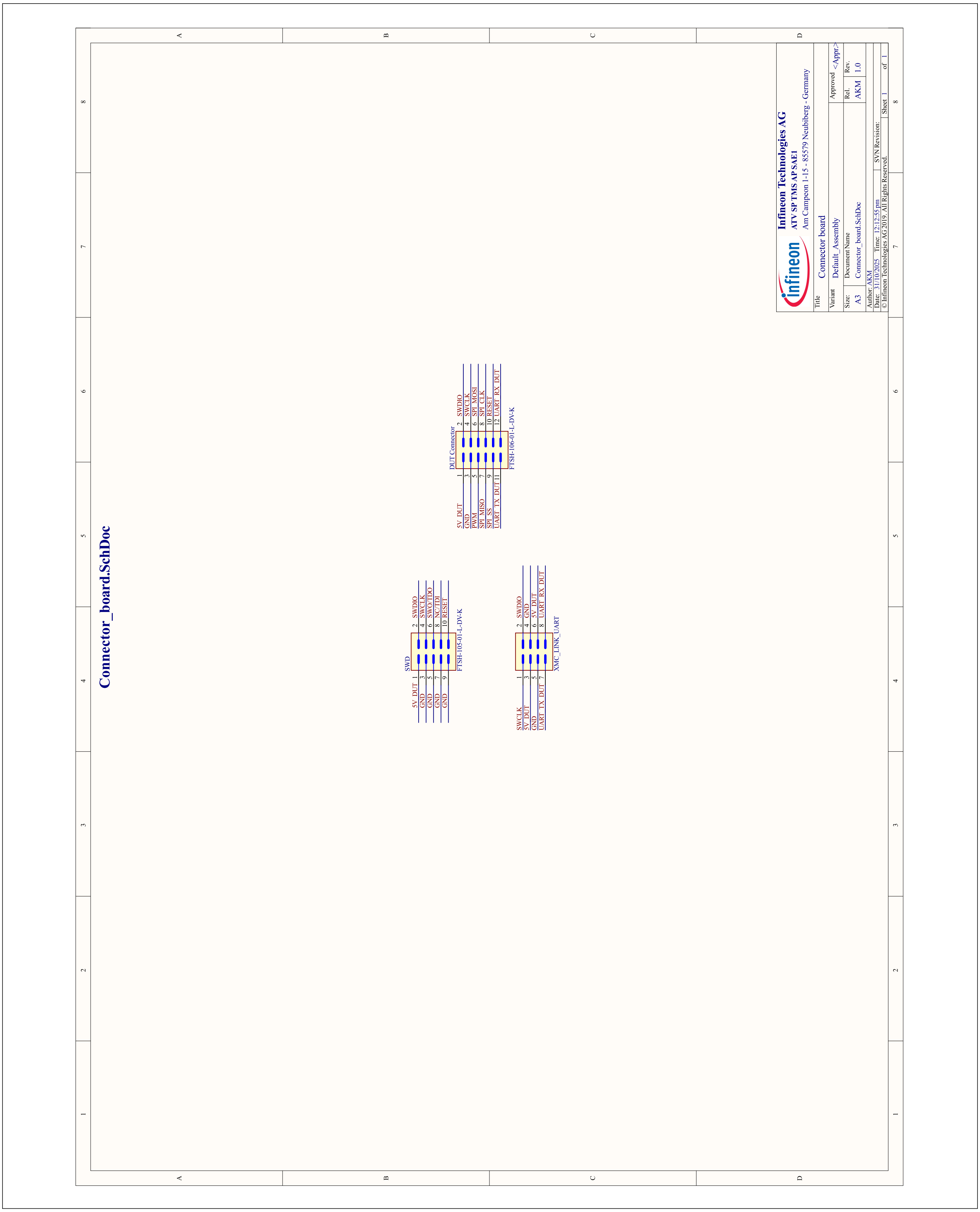

Figure 46 **Connector board**

8.2 Bill of materials

Table 2 **Bill of materials**

Designator	Value	Description	Quantity	Manufacturer order number	Manufacturer	Automotive qualified
B1		XENSIV™ Cost Optimized Miniature TMR Current Sensor	1	TLE5572-AE24E1-R-E0001	Infineon Technologies	AEC Q100
C1, C_LIN2	220pF		2	CGA3E2C0G1H221J080AA	TDK Corporation	AEC Q200
C2	100nF		1	GCM155R71H104KE02	Murata	AEC Q200
C3, C6, C7, CPI1, CPI2, CPI5, CPI6, CVS2	4.7uF		8	GRT21BC71H475KE13L	Murata	AEC Q200
C5	150uF		1	EEHZL1E151V	Panasonic	AEC Q200
C_DC1, CRP1	100nF		2	CGA3E3X8R1H104K080AB	TDK Corporation	AEC Q200
CCP1, CCP2	220nF		2	GCM188R71H224KA64	MuRata	AEC Q200
CPI3, CPI4	100nF		2	GCM188L81H104KA57	MuRata	AEC Q200
CVCPH1	470nF		1	CGA3E3X7R1H474K080AE	TDK Corporation	AEC Q200
CVDDP1, CVS1, CVSNS1	100nF		3	CGA2B3X7R1H104K050BB	TDK Corporation	AEC Q200
CVSCP1	1uF		1	CGA3E3X5R1H105K080AB	TDK Corporation	AEC Q200
CVSNS2	1uF		1	CGA3E1X7R1C105K080AC	TDK Corporation	AEC Q200
D_CP1	30V	Schottky Barrier Quadruple Diode, 30V, 200mA	1	BAT54XY,115	Nexperia	AEC Q101
DRP1	30V	Medium Power AF Schottky Diode	1	BAS3010B-03W	Infineon Technologies	AEC Q101
DVS1	BAS52-02V	Silicon Schottky Diode	1	BAS52-02V	Infineon Technologies	AEC Q101

(table continues...)

Table 2 (continued) Bill of materials

Designator	Value	Description	Quantity	Manufacturer order number	Manufacturer	Automotive qualified
L1	1.2uH		1	78439344012	Wurth Elektronik	AEC Q200
Q1	IAUZN04S7N026	OptiMOS™ 7 Power Transistor, 114A, 40V	1	IAUZN04S7N026	Infineon Technologies	AEC Q101
QRP1	BC817-40LT1G	Bipolar (BJT) Transistor NPN 45V 500mA	1	BC817-40LT1G	ON Semiconductor	No
R1, R9	4.7k		2	CRCW04024K70FK	Vishay	AEC Q200
R2, R3, R4, R5, R6, R7	100R		6	CRCW0402100RFK	Vishay	AEC Q200
R8, R_LIN1	0R		2	ERJ2GE0R00X	Panasonic	AEC Q200
RRP1	3.3k		1	CRCW04023K30FK	Vishay	AEC Q200
RRP2	10k		1	CRCW040210K0FK	Vishay	AEC Q200
RTB1	47R		1	CRCW060347R0FK	Vishay	AEC Q200
RVSCP1	2R		1	CRCW06032R00FK	Vishay	AEC Q200
TRACEBOX1		Connector Header Surface Mount 12 position 0.050 (1.27mm)	1	FTSH-106-01-L-DV-K	Samtec	No
U_TLE1		Microcontroller with LIN and Motor Driver for BLDC Application	1	TLE9954QSW40-33	Infineon Technologies	AEC Q100

8.3 Layout

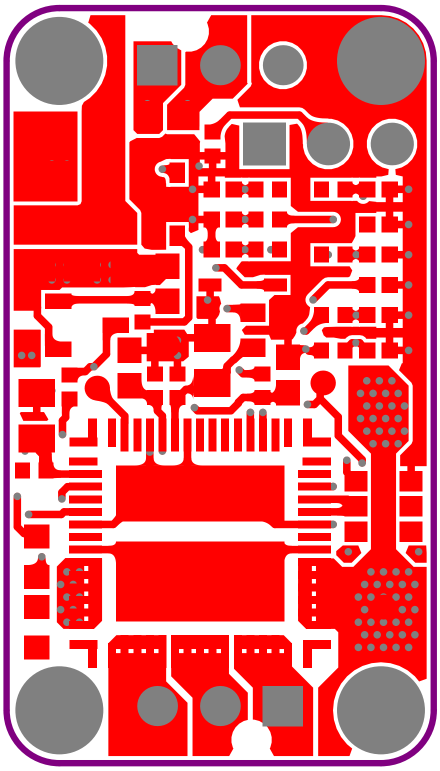

Figure 47 Top layer

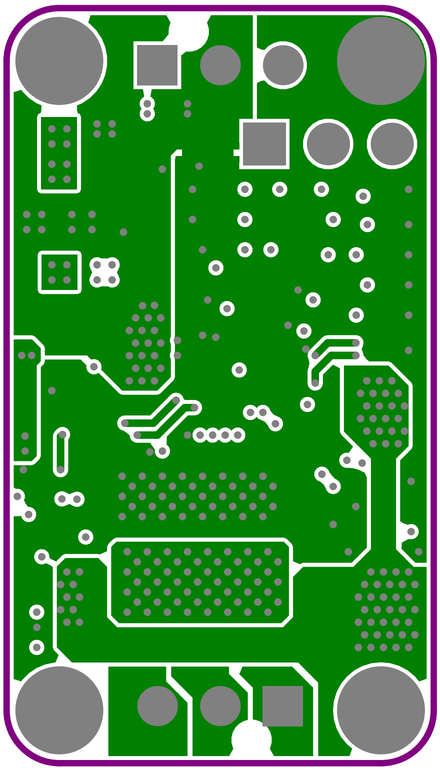

Figure 48 Layer 2

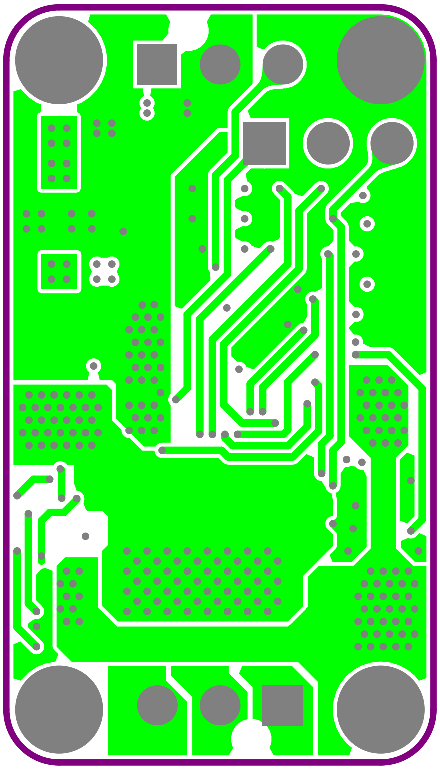

Figure 49 Layer 3

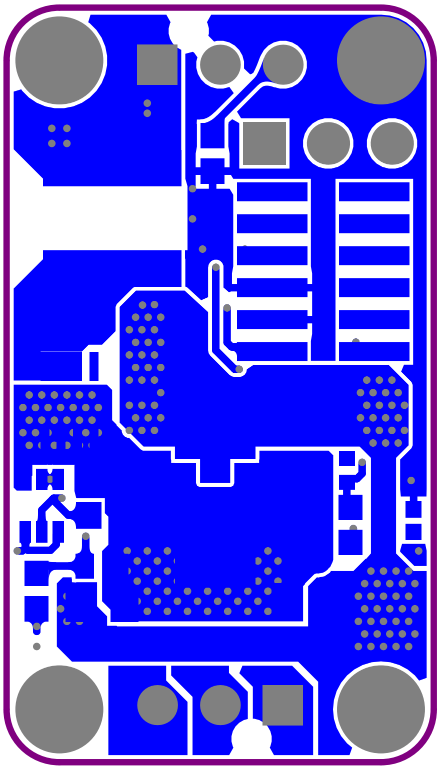

Figure 50 Bottom layer

Glossary

ADC

analog-to-digital converter (ADC)

BLDC motor

brushless DC motor (BLDC motor)
A synchronous motor using a direct current electric power supply.

BLDC

brushless direct current (BLDC)

DC

direct current (DC)

One-directional flow of electric charge. An electrochemical cell is a prime example of DC power. Direct current may flow through a conductor such as a wire, but can also flow through semiconductors, insulators, or even through a vacuum as in electron or ion beams. The electric current flows in a constant direction, distinguishing it from alternating current (AC).

EMC

electromagnetic compatibility (EMC)
The ability of electrical equipment and systems to function acceptably in their electromagnetic environment, by limiting the unintentional generation, propagation and reception of electromagnetic energy which may cause unwanted effects such as electromagnetic interference (EMI) or even physical damage in operational equipment.

GND

ground (GND)

GPIO

general purpose input output (GPIO)

GUI

graphical user interface (GUI)

An interface that enables users to interact with electronic devices through icons and visual indicators.

LIN

local interconnect network (LIN)

MCU

microcontroller unit (MCU)

A small computer on a single integrated circuit containing a processor core, memory, and programmable input/output peripherals.

PCB

printed circuit board (PCB)

A board that mechanically supports and electrically connects electronic components using conductive tracks, pads, and other features etched from copper sheets laminated onto a non-conductive substrate.

PWM

pulse-width modulation (PWM)

A technique to encode an analog value into the duty cycle of a pulsing signal with arbitrary amplitude.

TMR

tunnel magnetoresistance (TMR)

A magnetoresistive phenomenon that occurs in a magnetic tunnel junction, used for example, for sensors.

Revision history

Document version	Date of release	Description of changes
Rev. 1.00	2026-03-06	• Initial document release

Trademarks

All referenced product or service names and trademarks are the property of their respective owners.

Edition 2026-03-06

Published by

Infineon Technologies AG

81726 Munich, Germany

Do you have a question about any aspect of this document?

Email: erratum@infineon.com

Document reference
IFX-odo1772181697214